University of New Mexico
UNM Digital Repository

Biomedical Engineering ETDs | Engineering ETDs

7-13-2015

ANALYSIS OF PROTEASE ACTIVITY USING MEMBRANE- COATED BIOMIMETIC MICROSPHERES

Jennifer M. Fetzer

Follow this and additional works at: https://digitalrepository.unm.edu/bme_etds

Recommended Citation
Fetzer, Jennifer M.. "ANALYSIS OF PROTEASE ACTIVITY USING MEMBRANE- COATED BIOMIMETIC MICROSPHERES." (2015). https://digitalrepository.unm.edu/bme_etds/4

This Thesis is brought to you for free and open access by the Engineering ETDs at UNM Digital Repository. It has been accepted for inclusion in Biomedical Engineering ETDs by an authorized administrator of UNM Digital Repository. For more information, please contact disc@unm.edu.

www.manaraa.com

Jennifer M. Fetzer

Candidate

Biomedical Engineering

Department

This thesis is approved, and it is acceptable in quality and form for publication:

Approved by the Thesis Committee:

Dr. Andrew P. Shreve, Chairperson

Dr. Steven Graves

Dr. Gabriel Montaño

www.manaraa.com

ANALYSIS OF PROTEASE ACTIVITY USING MEMBRANE-COATED BIOMIMETIC MICROSPHERES

By

JENNIFER M. FETZER

B.S. BIOLOGY, UNIVERSITY OF NEW MEXICO, 2012

M.S. BIOMEDICAL ENGINEERING, UNIVERSITY OF NEW MEXICO, 2015

THESIS

Submitted in Partial Fulfillment of the
Requirements for the Degree of

Master of Science

Biomedical Engineering

The University of New Mexico
Albuquerque, New Mexico

July, 2015

www.manaraa.com

ACKNOWLEDGEMENTS

The work presented in this thesis was made possible by the help and mentorship of many individuals. First and foremost, I would like to express my gratitude to my advisor, Dr. Andrew Shreve, for allowing me to work in his research group at UNM and for the patience and guidance he has provided over the past two years. I am also extremely grateful for the help provided by my co-advisor, Dr. Steven Graves, and our Los Alamos National Labs colleague, Dr. Gabe Montaño, for serving on my defense committee and providing me with invaluable advice and guidance on this project.

I am deeply indebted to my postdoc mentor, Dr. Nesia Zurek, for her countless hours of discussion and training in the lab regarding this work. I would also like to thank Dr. Carl Brown, who helped develop the protocols for getting this project started. Additionally, the purification of SNAP-25 T-Sapphire would not have been possible without the aid of Dr. Arjun Thapa, who generously donated his time to help me with the work presented in this thesis.

I would also like to thank all of the students in the Shreve and Graves labs, who have supported me and provided me with help on this project the past two years. Specifically, José Cornejo, who provided invaluable suggestions as his project was the foundation for this work. Additionally, Lennae Ismari purified the SNAP-25 GFP that was used in these experiments.

A big thanks goes out to Matt Rush, Jacqueline Delora, Kent Coombs, Jaime Juarez, Ian Young, and Aaron Jenkins for tediously proofreading my thesis and providing input for my defense presentation.

Finally, I would like to acknowledge all of my family and friends who provided endless support throughout my graduate career.

www.manaraa.com

ANALYSIS OF PROTEASE ACTIVITY USING MEMBRANE-COATED BIOMIMETIC MICROSPHERES

By

Jennifer M. Fetzer

B.S. Biology, University of New Mexico, 2012

M.S. Biomedical Engineering, University of New Mexico, 2015

ABSTRACT

Poisoning by Botulinum Neurotoxins (BoNTs) leads to the severe neuroparalytic illness known as botulism, which is characterized by flaccid paralysis, respiratory failure, and death. BoNTs are the most acutely toxic substances on the planet, so detection at physiologically relevant concentrations is difficult. Because current treatments for botulism cannot reverse existing paralysis, rapid detection is key, and current diagnostic techniques are not meeting this need. We have developed a flow-based assay platform that allows for detection of the Light Chain of BoNT/A as well as a means to study the action of the toxin on its protein substrate in a system that mimics many aspects of a physiologically relevant environment. The total assay time has been reduced to approximately 20 hours, and this platform has multiplex and high throughput screening capabilities for drug discovery.

www.manaraa.com

TABLE OF CONTENTS

www.manaraa.com

www.manaraa.com

Chapter 1

INTRODUCTION

1.1 Overview and Project Aims

Botulism is a severe neuroparalytic disease, and the extreme lethality of Botulinum Neurotoxins (BoNTs) make detection of the toxin challenging. The lethal dose of BoNTs is very low (1 ng/kg), so it is difficult to measure the presence of the toxin at physiologically relevant concentrations. In fact, current diagnostics often rely on observing the onset of paralytic symptoms in the patient [1]. For effective therapy, however, early detection is critical. Thus, there is a need for fast, accurate *in vitro* assays capable of BoNT detection.

Previous work by Graves and coworkers has demonstrated that a microsphere-based assay can be used to measure the presence of BoNT proteolytic activity. [2] However, this existing approach does not present the BoNT substrate in its fully natural, membrane-associated state, and therefore cannot investigate the role played by membranes in controlling BoNT activity. This limitation could be an important factor in both the detection of BoNT enzymatic activity and in the use of this technology for drug-discovery screening.

The research reported in this thesis outlines steps towards the development of a biomimetic, membrane-containing microsphere-based protease assay that can detect the presence of BoNT/A using flow cytometry. By tagging a full-length membrane-bound SNAP-25 protein substrate with a fluorophore located downstream of the BoNT/A cleavage site, proteolytic cleavage can by observed via loss of fluorescence after incubation with the toxin. Although not included in

www.manaraa.com

this study, these microsphere-based assays have the potential to be multiplexed for cross-reactivity studies and are also capable of high throughput screening for drug discovery purposes. Furthermore, there is much that is still unknown about the interaction between BoNTs and SNARE proteins, and we hypothesize that the membrane plays an important role in facilitating these interactions. Unlike current BoNT detection systems, this assay design incorporates a lipid membrane in an effort to better mimic a biologically relevant environment. Relevant background information is presented in the remainder of this chapter, while the overall thesis describes progress towards the goal of implementing a flow-based assay for BoNT activity against membrane-bound substrates.

1.2 Membrane Docking and Vesicle Fusion

The SNARE (soluble N-ethylmaleimide-sensitive fusion protein attachment receptors) protein complex mediates cell-cell communication via the highly coordinated trafficking and fusion of vesicles with a target compartment, allowing neurotransmitter release [3]. The three SNARE proteins that are integral to membrane fusion and docking are SNAP-25, VAMP, and syntaxin. SNAP-25 (25 kDa synaptosome-associated protein) is a soluble protein anchored in the plasma membrane by palmitoyl groups attached to four cysteine residues on the molecule [4]. VAMP (vesicle-associated membrane protein, also termed synaptobrevin) is the integral synaptic vesicle membrane protein that contains a COOH transmembrane domain that inserts into the vesicle bilayer [4,5]. Finally,

www.manaraa.com

syntaxin is a type II membrane protein that contains four α-helical regions and is anchored to the membrane by a COOH-terminal transmembrane domain [4,5].

When these three proteins bind, they create a coiled four-helix bundled SNARE complex. X-Ray crystallography and deep-etch electron microscopy show that two SNAP-25 helices, one VAMP helix, and one syntaxin helix intertwine in a parallel fashion (with all N-termini at the same end of the bundle) to form this extremely stable four-helical core complex [6–10]. The free energy release during formation of this four-helix bundle is enough to drive membrane fusion (Figure 1.1) [4,5]. The widely accepted mechanism of fusion is that there is a Ca^{2+} triggered 'zippering' effect of the SNARE motifs from the N termini to the C-terminal membrane anchors, and this effect clamps the membranes together. The mechanical forces during clamping are thought to be sufficient to overcome the energy barrier for fusion, though the details of this mechanism are still unclear [3].

After the fusion event occurs, the presynaptic vesicles are able to release their contents into the synaptic cleft [6]. This overall process is essential for nervous system function and health, as membrane fusion must be achieved for chemical synaptic transmission to occur [6]. In the case of the SNARE protein complex, acetylcholine-filled presynaptic vesicles fuse with the plasma membrane and release their contents into the synaptic cleft. This acetylcholine (ACh) can then bind receptors on skeletal muscle fibers and initiate muscle contractions [6,10].

www.manaraa.com

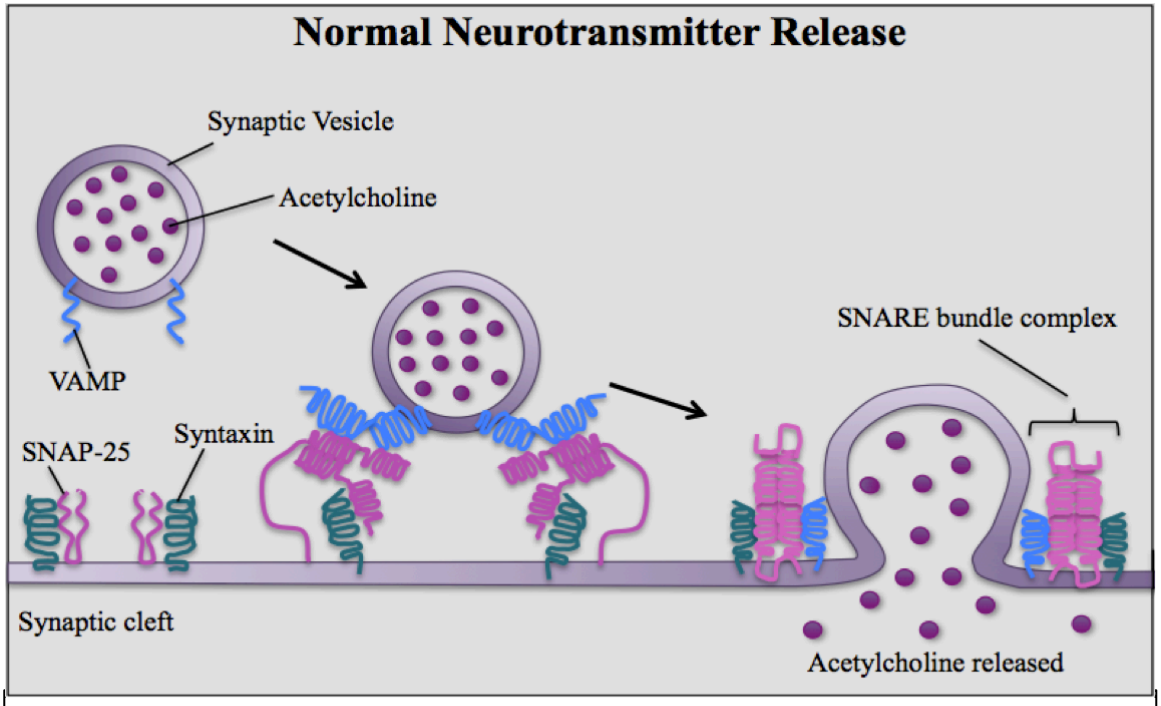

Figure 1.1 Mechanism of normal neurotransmitter release via vesicle docking and membrane fusion. The SNARE bundle complex is formed by the binding of syntaxin, synaptobrevin (also termed VAMP), and SNAP-25. This fusion allows for the release of acetylcholine into the synaptic cleft at the neuromuscular junction. Figure adapted from Binz *et al.* (2010) [11].

www.manaraa.com

After the vesicle contents are released, a recycling pathway is initiated where the SNARE core complex is disassembled into its monomeric components. This disassembly is dependent on ATP and the adaptor protein α-SNAP (soluble NSF attachment protein) [6]. Because the four-helix SNARE bundle is exceptionally stable, disassociation requires a large amount of metabolic energy. This energy is provided by N-ethylmaleimide sensitive fusion protein (NSF), which is recruited by bound α-SNAP [3,6]. Subsequent hydrolysis of ATP by NSF causes dissociation of the SNARE complex and vesicle exocytosis [6,7]. By this mechanism of vesicle docking/fusion and recycling, neurotransmission is achieved and nervous system function is maintained.

1.3 Proposed Mechanism of SNARE Cleavage by BoNTs

The botulinum neurotoxin (BoNT) is one of the most toxic substances known, with a 50% lethal dose for susceptible humans of approximately 1 ng/kg of body weight [11,12]. BoNTs are secreted by the anaerobic bacterium *Clostridium botulinum* and are composed of a heavy chain (~100 kDa) and light chain (~50 kDa) [5,11,13,14]. The toxins are ingested and taken up by epithelial cells, where they eventually reach the motor nerve terminals [11]. They are then taken up by the recycling pathway of synaptic vesicles via four main steps: first, they bind to ganglions at the surface of nonmyelinated nerves. Second, there is an interaction with the synaptic vesicle receptors for BoNT/A (this process is heavy-chain mediated) [11]. Third, the vesicles are endocytosed, allowing intracellular transport. The acidic environment during transport causes the heavy chain to

www.manaraa.com

undergo a conformational change and form a cation-selective channel. This pore formation is thought to facilitate the passage of the catalytic domain from the membrane into the cytosol [1]. The light chain also partially unfolds during this step [11]. Finally, the light chain is released from the heavy chain to hydrolyze peptide bonds of SNARE proteins in the cytosol. Each of the seven serotypes of BoNT (A-G) have a unique specificity to its respective SNARE protein substrate [14]. BoNT/A, for example, proteolyzes SNAP-25 by hydrolyzing the peptide bond nine amino acids away from the C-terminus of the protein [11]. The BoNT/A cleavage site and overall structure of SNAP-25 are shown in Figure 1.2.

The light chain of botulinum neurotoxin contains a highly conserved Zn^{2+} His-Glu-X-X-His binding motif, indicating that the proteolytic activity of BoNTs is zinc-dependent [11]. Zn^{2+} ions are coordinated by the two histadines in this motif, a water molecule that is bonded to the glutamate residue, and another Glu that is located 35 amino acids downstream [11]. The catalytic mechanism is not entirely known, but it is thought that the polar water molecule bonded to the Glu residue coordinates a nucleophilic attack on the nitrogen atoms in the peptide bond of the SNARE protein. Via this proteolytic mechanism, each of the seven serotypes of BoNT specifically cleaves its respective SNARE protein substrate, blocking neurotransmitter release and causing flaccid paralysis, respiratory failure, and death.

www.manaraa.com

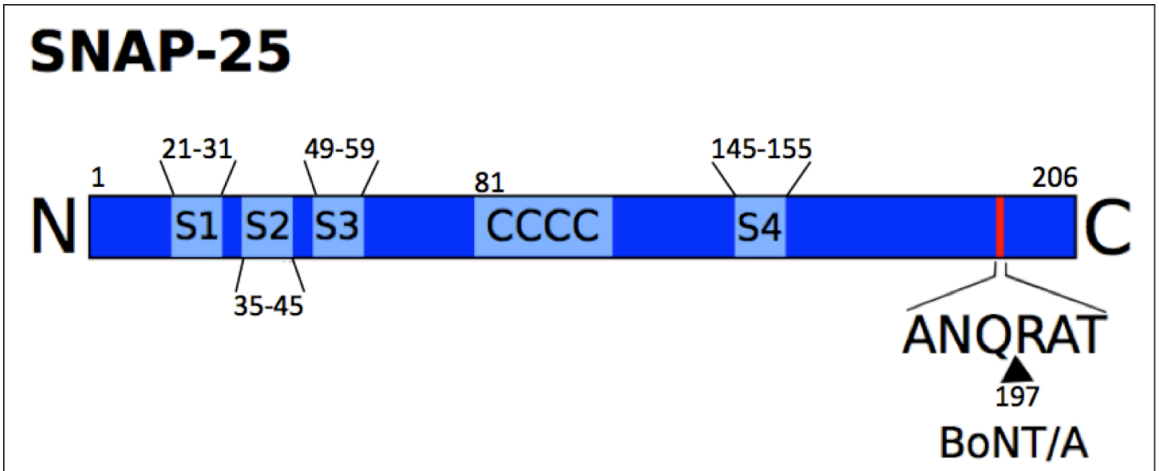

Figure 1.2 Structure of SNAP-25. The protease cleavage site for the BoNT/A is shown in red. The S1, S2, S3, and S4 domains represent the four copies of the nine-residue SNARE motif that is conserved amongst all three SNARE proteins. The protein is anchored to the membrane via the palmitoyl groups attached to the four cysteine residues (CCCC) in the middle of the protein. Figure adapted from Binz *et al.* (2010) [11].

www.manaraa.com

1.4 Overview of Flow-Based Assays

Microsphere-based flow cytometric assays have a wide variety of biomedical applications. Flow cytometry is a powerful tool that enables the analysis of multiple samples simultaneously, making cross-reactivity studies possible [15]. Modern flow cytometers are capable of analyzing thousands of particles per second in "real time." Because of this incredibly rapid analysis time, flow cytometry is also often used for high throughput screening and drug discovery studies [15]. Additionally, minimal sample volumes are required, and flow cytometry can yield highly reproducible results [15].

Flow cytometry works by using sheath fluid to hydrodynamically focus a sample stream into a very narrow channel [16]. The particles are focused into a single-file line, where they are individually interrogated by a laser beam [16]. When the laser beam hits the particle, two types of measurements are produced. First, a fluorescence measurement results from the emission light given off of the particles when excited by the particular wavelength of the laser. Second, the amount of light scattered from the particle is quantifiable and directly related to both the size and density of the particle (larger, denser particles will scatter more light than smaller particles) [16]. The light that is scattered in the forward direction (forward scatter) is more indicative of cell size, while the light that is scattered to the side (side scatter) is more indicative of density. These fluorescence and scatter measurements are collected by a detector, where they can then be analyzed using flow cytometry software. Figure 1.3 shows a schematic

www.manaraa.com

from Abcam depicting hydrodynamic focusing and particle interrogation in flow cytometry [16] .

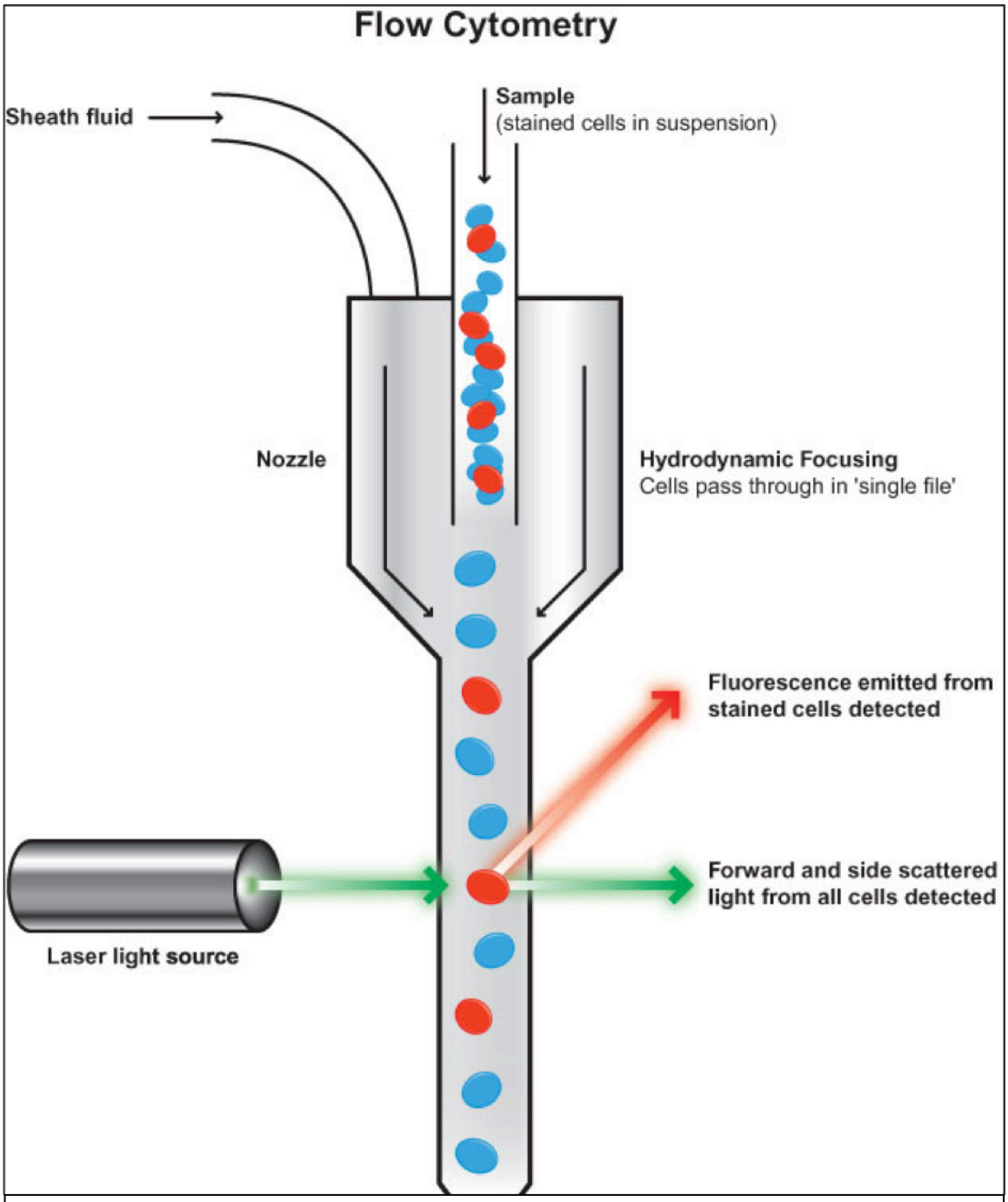

Figure 1.3 Illustration of hydrodynamic focusing and particle interrogation in flow cytometry. Figure from Abcam [16].

www.manaraa.com

1.4 Summary of Previous Research

Currently, the standard method (and only approved method) for positive confirmation of BoNTs is the mouse lethality bioassay, in which dilutions of the suspect material are injected into mice. The relationship between survival time and toxin concentration can then be plotted as a standard curve [1,12,17]. While this method has demonstrated a low limit of detection (LOD) in the picomolar range, it has many limitations [12]. First, this clinical diagnosis of botulism relies on the patient's development of symptoms, which limits the effectiveness of treatment [1]. Second, the mouse bioassay is labor intensive and takes two to four days to perform. The current treatment for botulism is the administration of equine antitoxin, which cannot reverse existing paralysis due to its inability to cross the nerve membrane and neutralize the toxin in already affected cells [1]. Because of this, early detection is key, and current methods do not meet the clinical need for an accurate and rapid diagnosis. Immunoassays such as ELISA can also be used for BoNT detection, but these assays are not high throughput, not capable of being multiplexed, and detect only the presence of BoNT without providing any information on the enzymatic activity of the neurotoxin [1,12]. A summary of the performance of current diagnostic techniques for BoNT is shown in Table 1.1.

www.manaraa.com

Techniques for Detection of *Clostridium botulinum* Neurotoxins				
Technique	**Limit of Detection (LOD)**	**Detection Time**	**Multiplex**	**Throughput**
Mouse lethality bioassay	20 pg/ml	4-6 days	No	Low
ELISA	100 pg/ml	5-6 hours	No	Mid
AuNPs	5 ng/ml	4 hours	No	Mid
Cellular assay	nM to pM	2-3 days	No	Low

Table 1.1 Summary of current techniques for BoNT detection. Table adapted from Cai *et al.* (2007) [1].

Many *in vitro* methods for BoNT detection are under development, but none have yet been approved for clinical use [17]. For example, gold nanoparticles (AuNPs) have been biofunctionalized with peptides that mimic SNAP-25. The proteolytic cleavage of these peptides by BoNT/A alters how the AuNPs aggregate, leading to changes in how the nanoparticles interact with light, so BoNT detection can be achieved by colorimetric sensing [12]. While this assay greatly reduces detection time for BoNT/A compared to the mouse lethality assay (the overall assay time is about 4 hours), it does not incorporate a full-length SNAP-25 substrate or a lipid membrane, so it is limited in terms of providing information on how the protease acts on a membrane protein in a fully

www.manaraa.com

biologically relevant environment. Cellular-based assays are also utilized for BoNT detection. PC-12 neuronal cells or spinal chord cultures can be used to monitor the inhibition of neurotransmitter release when exposed to BoNTs [1]. While this method does provide information on the overall enzymatic activity of BoNTs in a physiologically relevant environment, it also has many disadvantages. First, these cell-based assays take at least 2-3 days to perform, which again limits the need for rapid diagnosis. Maintaining the cell lines is also both labor-intensive and expensive, and the assay itself is complicated and difficult to perform [1]. Cellular assays are also low throughput and incapable of multiplex studies.

The flow-based assay platform described in this thesis addresses many of the limitations of current BoNT detection techniques. First, the required detection time is significantly shorter than many of the current techniques, with the entire assay taking approximately 24 hours. Second, it is the only membrane-containing method available that is capable of both multiplexing and high throughput screening, allowing the possibility of cross-reactivity studies and drug screening capabilities. Because the membrane may play an important role in mediating BoNT activity, it is important to incorporate a lipid bilayer to better resemble a biological environment when doing drug screening and detection studies.

Previous research by Graves and coworkers used biotinylated, full-length SNAP-25 directly bound to streptavidin microspheres for BoNT/A Light Chain (LC) detection via flow cytometry [2]. The SNAP-25 protein is tagged with a fluorescent molecule at the C terminus (after the protease cleavage site), so the presence of BoNT is indicated by loss of fluorescence once the protease cleaves

www.manaraa.com

off this fluorophore [2]. This assay design is described in detail in Chapter 3. While this previous microsphere-based assay platform is capable of high-throughput screening and multiplex studies, it still lacks a lipid membrane. Because SNARE proteins are all either membrane or membrane-associated proteins, we hypothesize that the membrane plays a critical role in facilitating the interaction between BoNTs and SNARE protein cleavage. In order to better mimic a natural environment, we propose to develop a microsphere-based protease assay for detection of BoNT/A LC that incorporates a full-length SNAP-25 substrate and a lipid membrane. Our expectation is that this system will provide a means to detect BoNT activity against substrates presented in a more natural environment and also provide a means to study the role played by membranes in mediating the overall neurotoxin activity.

1.6 Overview of Thesis

In the remainder of this thesis, the following results are presented. Chapter 2 describes the construct designs, expression, and purification of the two full-length SNAP-25 constructs used in this study: SNAP-25 GFP and SNAP-25 T-Sapphire. The membrane-based assay design, experimental methods, initial assay results using SNAP-25 GFP, and data analysis methods are all described in Chapter 3. Finally, a summary of this research and indication of future work are presented in Chapter 4.

www.manaraa.com

Chapter 2

SNAP-25 CONSTRUCT DESIGNS AND PURIFICATION

2.1 Introduction

Two constructs of full-length SNAP-25 were used in this study. The first construct is tagged with green fluorescent protein (GFP) at the C terminus. GFP was initially chosen as the detection fluorophore for these assays for several reasons. First, an extensive body of literature exists that use full-length SNAP-25 tagged with GFP, and this construct has been shown to be very stable under physiological conditions [4,18,19]. Second, biotinylated SNAP-25 GFP has been used historically in the Graves lab [2], so the SNAP-25 GFP plasmid was already synthesized and readily available in UNM's Center for Biomedical Engineering. The majority of the data presented in this thesis uses the biotinylated SNAP-25 GFP construct. However, in an important new direction, progress is underway to move to a new chromophore, T-Sapphire (TS). The TS fluorophore is a GFP mutant with many advantages over GFP. The four amino acid mutations that create TS (Q69M\C70V\V163A\S175G) facilitate improved folding relative to GFP while maintaining a comparable quantum yield, extinction coefficient, and pKa [20]. Additionally, TS has a Stokes Shift approximately 5 times larger than that of GFP (112 nm compared to 21 nm). Because the ability to distinguish between excitation and emission light is imperative in fluorescence-based studies, a larger Stokes Shift is preferable. Also, the use of TS allows use of the deep blue

www.manaraa.com

and UV excitation sources found on many commercial cytometers. Figure 2.1 compares the GFP and T-Sapphire spectra.

In this chapter, the construct designs, expression, and purification of both SNAP-25 GFP and T-Sapphire are described. Because SNAP-25 TS is a new construct, the purification process has required, and is still undergoing, a great deal of optimization. Initial attempts at purification are presented in this chapter, and preliminary data that shows binding of the SNAP-25 T-Sapphire protein to lipid-coated microspheres is shown in Chapter 4. Again, the majority of the experiments presented in the following chapters are carried out using the SNAP-25 GFP construct, which will lay the groundwork for future, detailed comparison of the performance of these two proteins.

www.manaraa.com

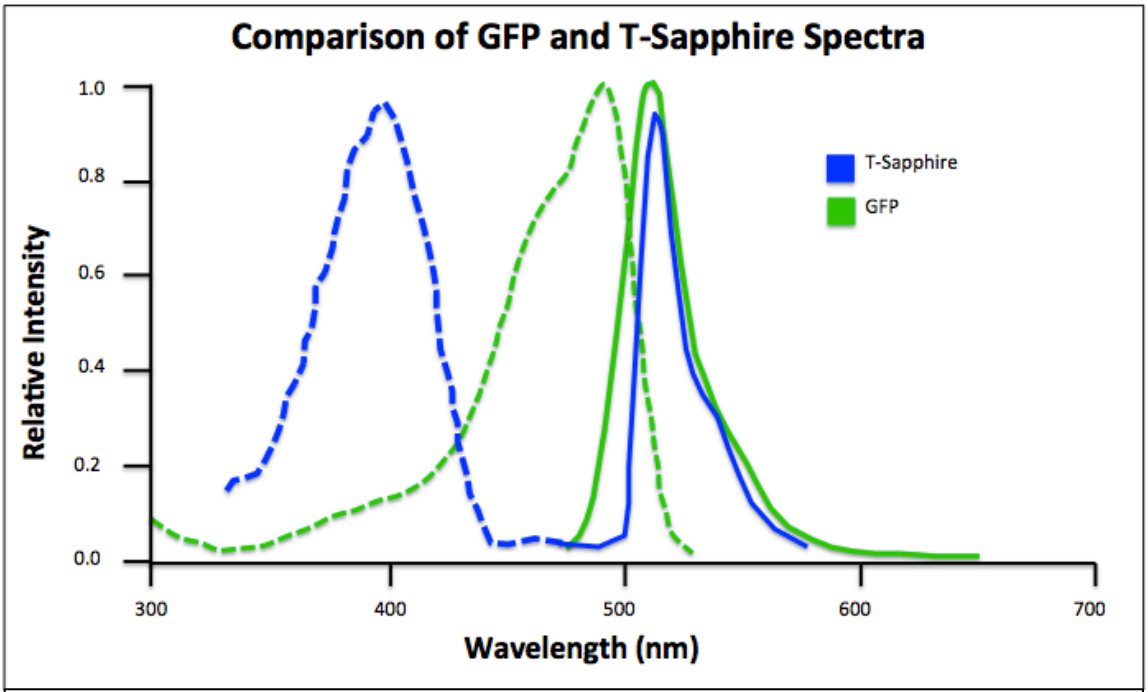

Figure 2.1 Spectral comparison of T-Sapphire (blue) and GFP (green). The dashed lines represent excitation and the solid lines show emission. GFP is excited optimally near 488 nm and emits at 509 nm, while T-Sapphire is excited optimally near 399 nm and emits at 511 nm. Figure adapted from Zapata-Hommer *et al.* (2003) [20].

www.manaraa.com

2.2 Purification of SNAP-25 GFP

2.2.1 SNAP-25 GFP Construct Design

The SNAP-25 GFP plasmid was made previously by the Graves group and coworkers. The EGFP was cut from the pEGFP-N2 plasmid (Clonetech) using the restriction enzymes BamHI and SacI [2]. The full-length SNAP-25 construct was cloned in a SNAP-25 clone plasmid (Open Biosystems) using polymerase chain reaction, and the ligated PCR product was also digested with BamHI and SacI [2]. This SNAP-25 was then inserted into the PinPoint Xa-1 vector (Promega) between the biotin tag and the EGFP. This vector has a T7 promoter and is inducible with Isopropyl β-D-1-thiogalactopyranoside (IPTG). The plasmid contains a gene for ampicillin (or carbenicillin (CARB)) resistance [2]. Figure 2.2 depicts a map of the SNAP-25 GFP plasmid and its features (figure made using SerialCloner). The complete plasmid sequence is listed in the appendix [2,21].

www.manaraa.com

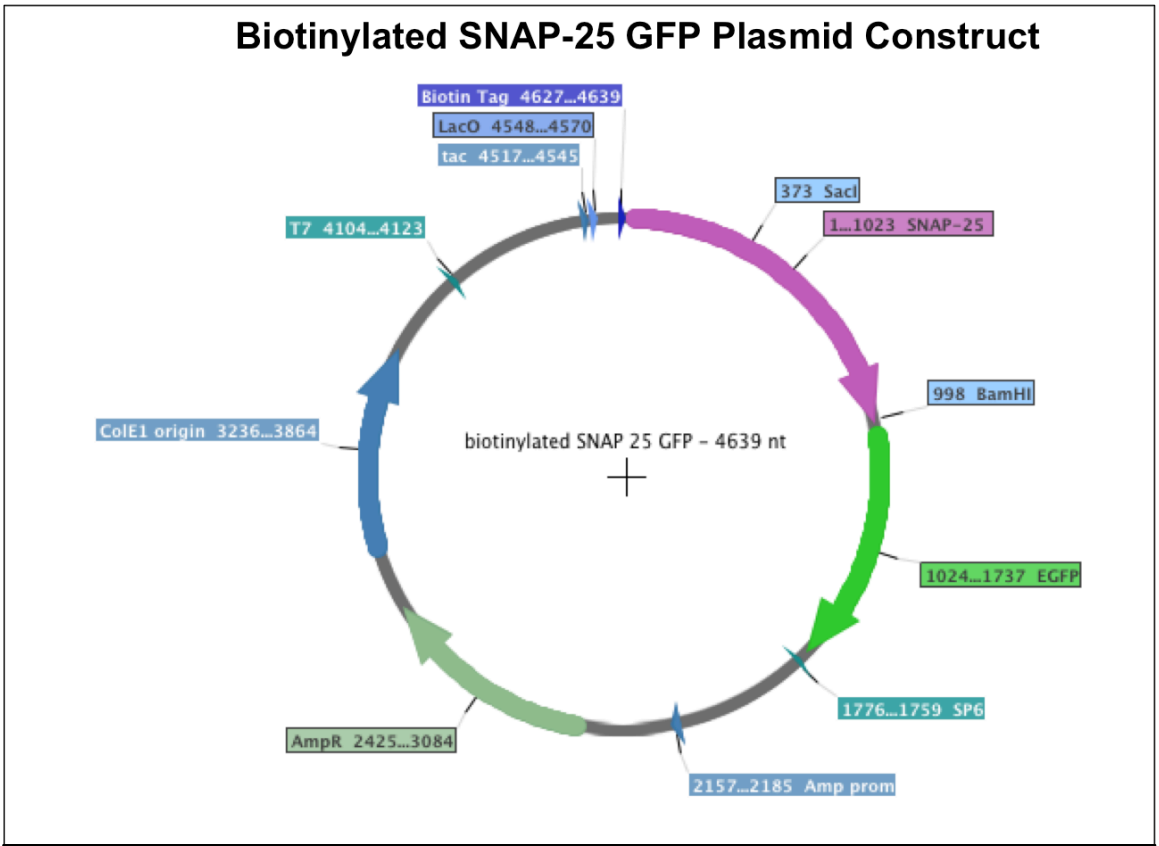

Figure 2.2 Map of the full-length SNAP-25 GFP plasmid in the Pinpoint Xa-1 vector. The SNAP-25 sequence (pink) is located between the biotin tag (dark blue) and the EGFP (light green). Figure made using SerialCloner.

www.manaraa.com

2.2.2 Transformation and Expression

The SNAP-25 GFP plasmid was transformed into competent AVB-101 *E. coli* cells from Avidity. This cell line was chosen for the expression of SNAP-25 GFP because it contains the pACYC184 plasmid (maintained by chloramphenicol (CAM)), which has been engineered to express an inducible BirA gene [17]. BirA is a biotin ligase that catalyzes *in vitro*, site-specific enzymatic biotinylation [17]. In other words, the AVB-101 cell line has been optimized for the expression of biotinylated proteins. While production of biotinylated protein is not essential for the present work, it was needed for the previous work that involved attachment of protein to streptavidin-coated microspheres [2]. Its use was continued here due to this past experience in protein expression and purification using this cell line and biotinylated protein.

The transformed bacteria were grown on Lysogeny Broth (LB) media plates containing 34 μg/ml of chloramphenicol (CAM) and 50 μg/ml CARB. A single colony from the transformation was collected and grown up in 3 ml of autoclaved Terrific Broth (TB) media (again containing 34 μg/ml of CAM and 50 μg/ml CARB) at 37°C overnight, shaking at 250 rpm. This overnight culture was then used to inoculate 250 ml of sterile TB media (with 34 μg/ml of CAM and 50 μg/ml CARB). 40 mM biotin was added, and the culture was allowed to grow for an additional 2-3 hours in the 37°C incubator, shaking at 250 rpm. When the OD_{600} reached a value of ~0.6, 100 μM of IPTG was added to induce the expression of the SNAP-25 GFP protein. After induction with IPTG, the

www.manaraa.com

temperature was reduced to 30°C, and the cells were grown overnight with the shaker on at 250 rpm.

After this overnight incubation, the cells were harvested by centrifugation at 3500 rpm for 30 minutes at 4°C. The supernatant was discarded, and the cell pellet was resuspended in 40 ml of sterile 1X Phosphate Buffered Saline (PBS) buffer (137 mM NaCl, 2.7 mM KCl, 10 mM Na_2HPO_4, 2mM KH_2PO_4, pH=7.4) and stored frozen at -20°C. Upon subsequent use, the resulting freeze-thaw cycle helps to lyse the cells.

2.2.3 **Purification on the FPLC**

The frozen cells in PBS were placed in a water bath at room temperature until thawed. One milliliter of a broad-spectrum protease inhibitor cocktail (Sigma-Aldrich) was added, and the solution was subsequently sonicated on the probe sonicator for 15 minutes at 10 Watts to sufficiently lyse the cells. The cell debris was extracted by centrifugation at 14,000 rpm for 30 minutes at 4°C. The supernatant was then loaded into the injection column of the FPLC for purification. The column contains SoftLink Avidin Resin (Promega), which binds the biotinylated SNAP-25 GFP. The bound protein was then eluted off of the column with a biotin elution buffer (1mM dithiothreitol (DTT) and 5mM biotin dissolved in PBS and vacuum filtered, pH=7.4). DTT is a reducing agent and helps ensure that the SNAP-25 GFP protein stays in the reduced form, thus preventing crosslinking. Elution fractions (tubes that demonstrated green fluorescence under UV illumination) were collected and spun down two times in

www.manaraa.com

molecular weight cut-off (MWCO) filter centrifuge tubes (EMD Millipore) for 12 minutes at 3500 rpm to further purify and concentrate the protein. Because the size of SNAP-25 GFP is ~62 kDa, a MWCO filter of 30 kDa was chosen. The protein retentate was then pipetted into dialysis tubing with a membrane MWCO of 6,000–8,000 Da. Four rounds of dialysis were performed at 4°C, switching out the dialysis buffer (3L of 50 mM HEPES and 100 mM NaCl, pH=7.4) every 4 hours. Protein purity was assessed by running a 10% SDS-PAGE protein gel (Figure 2.3). Finally, the protein concentration was measured using the A280 (i.e. the absorbance at λ= 280 nm) on the Nanodrop (Thermo Scientific).

www.manaraa.com

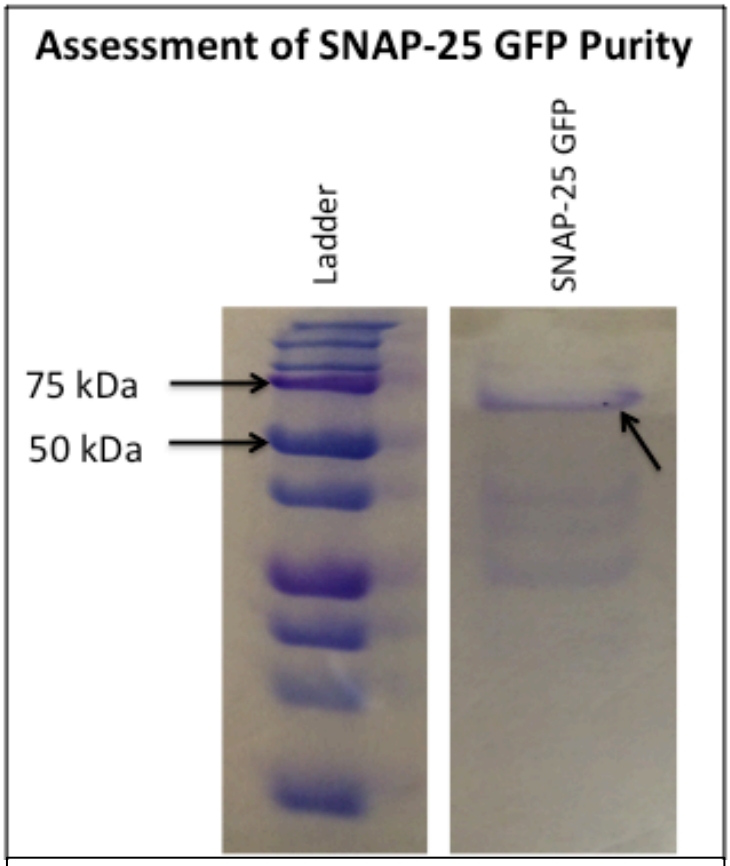

Figure 2.3 10% SDS-PAGE gel assessing the purity of SNAP-25 GFP (63.8 kDa) after purification on the FPLC and subsequent processing, as described in the text. The arrow indicates the protein of interest.

www.manaraa.com

2.2.4 Discussion

The amount of protein produced from the purification (as calculated from the A280 measurement on the Nanodrop) was 4 μM in a 2 ml volume. However, the SDS-PAGE gel in Figure 2.3 reveals that the SNAP-25 GFP protein is not completely pure (multiple protein bands are visible). These impurities can potentially be problematic downstream when trying to couple the SNAP-25 GFP to a lipid-coated microsphere. In order to address this concern and to minimize the effects of nonspecific binding, blocking steps with Bovine Serum Albumin (BSA) were incorporated into the coupling protocol (described in Chapter 3).

2.3 Purification of SNAP-25 T-Sapphire (TS)

2.3.1 SNAP-25 TS Construct Design

The SNAP-25 TS construct was designed in SerialCloner by mutating the 4 EGFP amino acids previously mentioned (Q69M\C70V\V163A\S175G) in the full-length SNAP-25 GFP construct to create the SNAP-25 T-Sapphire mutant. This sequence was inserted in the pET-15b vector (Novagen), which contains a His-tag coding sequence. This vector also has a T7 promoter and has bacterial resistance to ampicillin. The plasmid was prepared by GenScript. Figure 2.4 shows the SNAP-25 T-Sapphire plasmid and its relevant features. Copies of the plasmid were made using a MaxiPrep kit from QIAGEN, and a restriction digest was performed using the restriction enzyme BamHI to confirm that the plasmid was sequenced correctly. Figure 2.5 shows an acrylamide gel of the restriction digest.

www.manaraa.com

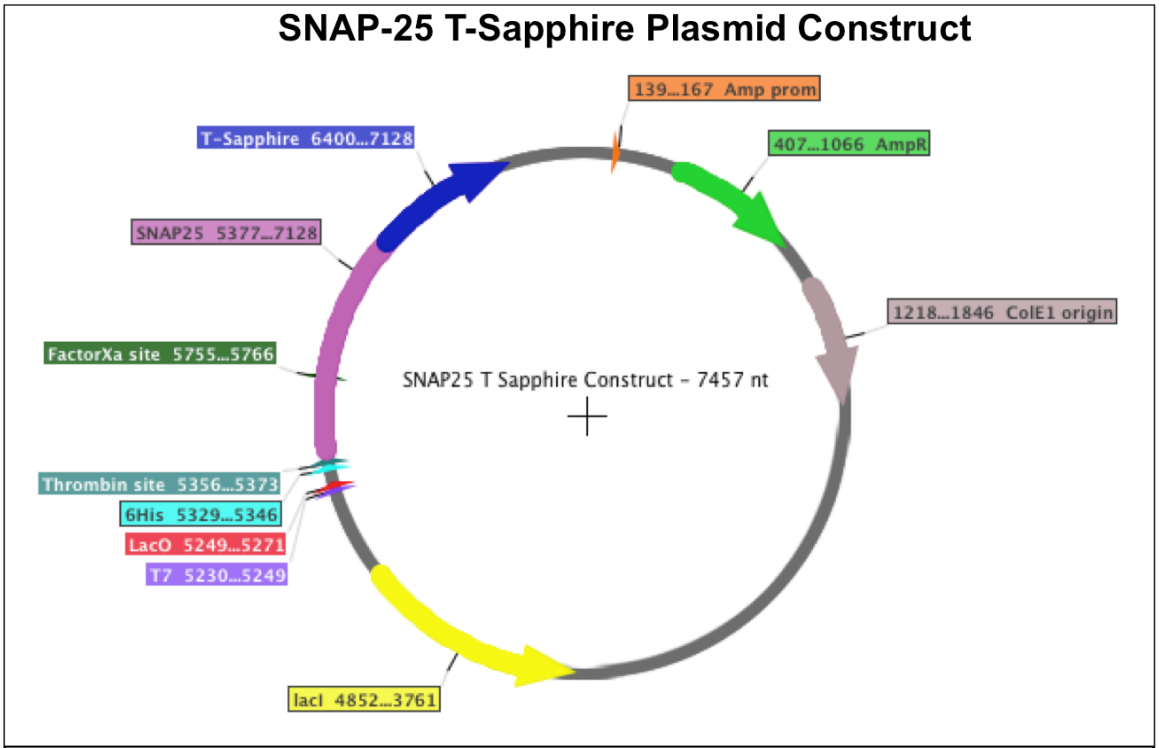

Figure 2.4 Map of the full-length SNAP-25 T-Sapphire plasmid in the pET-15b vector. The SNAP-25 sequence (pink) can be seen between the Histadine tag (light blue) and the T-Sapphire fluorophore (dark blue). Figure made using SerialCloner.

www.manaraa.com

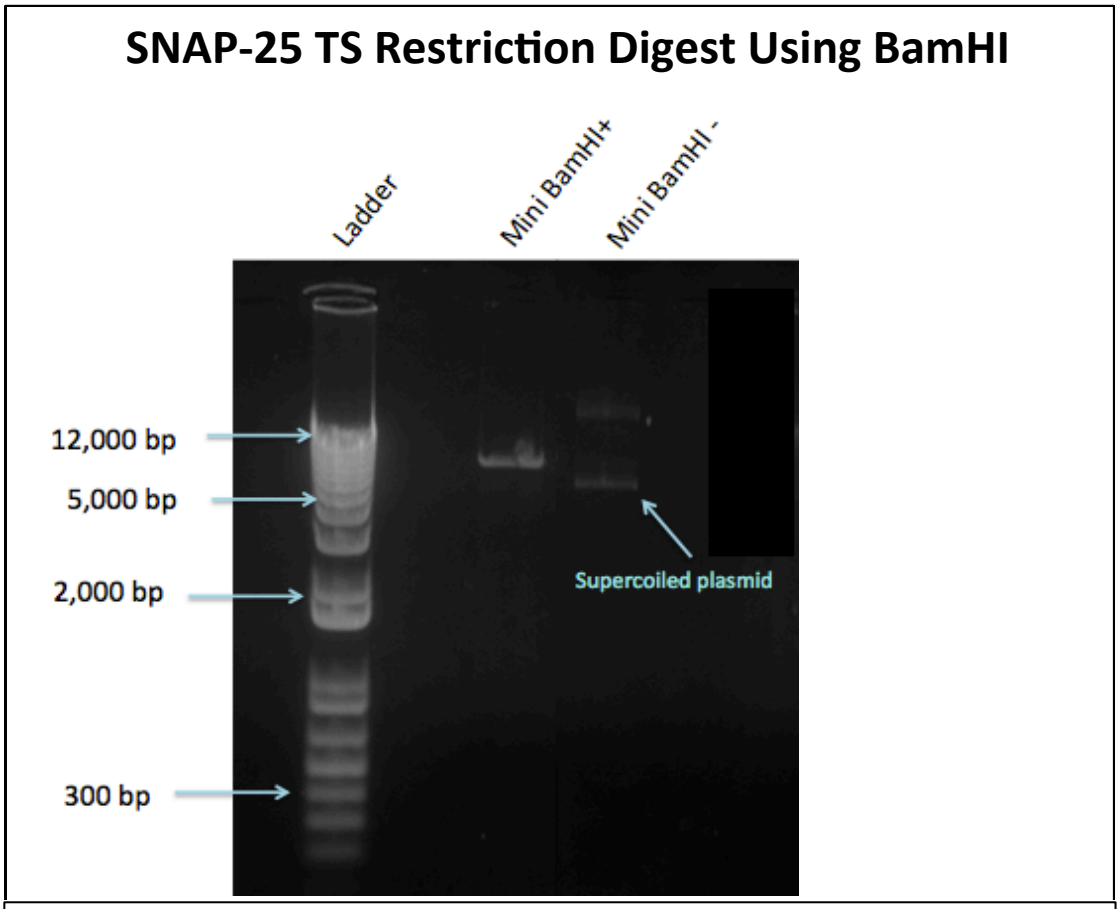

Figure 2.5 Restriction digestion analysis of SNAP-25 T-Sapphire plasmid incubated with BamHI. One fragment is generated at 7,457 bp. The Virtual Cutter tool in SerialCloner verified that this band is in the correct location for this reaction. The first lane (MiniBamHI +) contains the restriction enzyme, while the second lane (MiniBam HI -) is a negative control where the restriction enzyme was not added to the reaction.

www.manaraa.com

2.3.2 Transformation and Expression

The SNAP-25 TS plasmid was transformed into competent BL21 (DE3) pLysS *E. coli* cells (Promega). This cell line is very commonly used for protein expression of genes under control of a T7 promoter and contains the pLysS plasmid, which is maintained by CAM. The transformation and induction of the SNAP-25 TS plasmid were conducted under the exact same conditions and with the same antibiotics as the SNAP-25 GFP, with the exception that no biotin was added prior to induction (the SNAP-25 TS construct does not contain a biotin tag).

To ensure that the protein was being expressed, 1 ml aliquots of the cell culture were collected at various time points after induction and run on the PTI fluorometer to observe fluorescence (Figure 2.6). Before measurement on the fluorometer, the samples were diluted to obtain the same optical density at 600 nm. 24 hours after induction, an emission peak can be seen at 511 nm when exciting at 399 nm, which is the spectral signature of the T-Sapphire fluorophore.

After an overnight incubation at 30°C shaking at 250 rpm, the cells were harvested by centrifugation at 3500 rpm for 30 minutes at 4°C. The supernatant was discarded, and the cell pellet was stored at -20°C.

www.manaraa.com

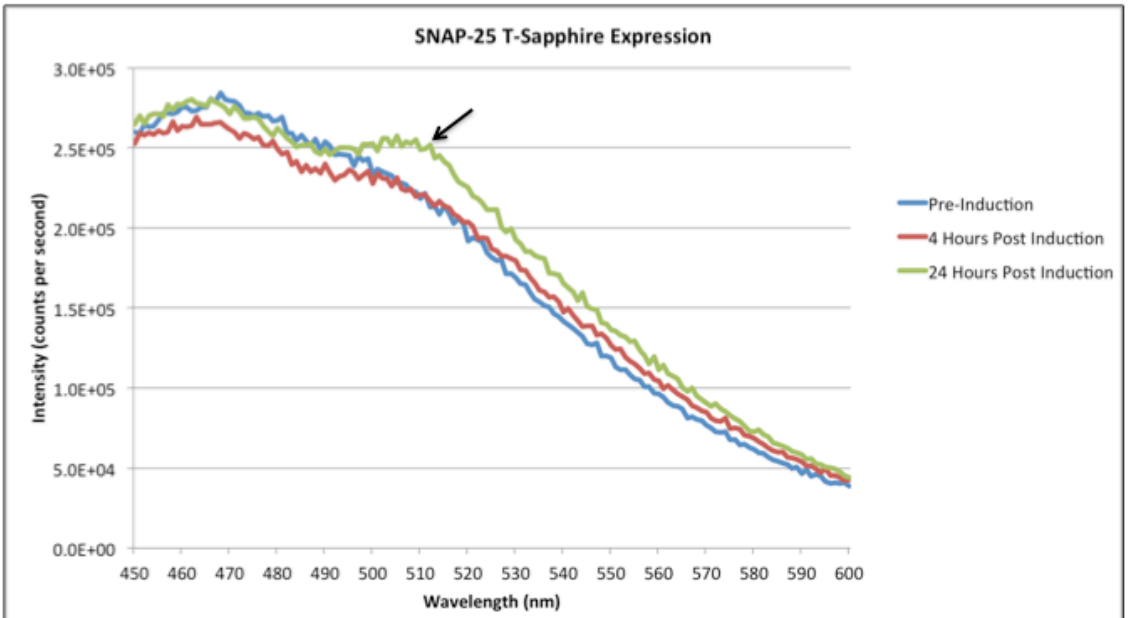

Figure 2.6 Emission scan of SNAP-25 TS samples taken at various time points after induction. Excitation for T-Sapphire is 399 nm, with an emission peak at 511 nm. The blue line represents the samples prior to induction, the red line is a sample four hours after induction, and the green line is 24 hours after induction. The arrow indicates the emission peak for the T-Sapphire fluorophore.

www.manaraa.com

2.3.3 Optimization of Buffering Conditions

As an initial step toward developing optimized purification protocols for SNAP-25-TS, various approaches were explored using 5 ml columns packed with Ni-NTA beads. These studies were carried out prior to FPLC purification described in Section 2.3.4. The primary objective of these initial studies was to optimize buffering conditions with the goal of minimizing the amount of nonspecific binding during purification. In order to reduce nonspecific binding, we needed to determine an optimal concentration of imidazole to use in the equilibration buffer.

The equilibration buffer flows through the column after the protein of interest has bound and is intended to wash away any other proteins that are nonspecifically bound to the column. Equilibration buffers were prepared with imidazole concentrations of 5 mM, 10 mM, and 20 mM in PBS (vacuum filtered, pH=7.4). One protease inhibitor tablet (Roche) was added to each buffer, as well as 2 mM beta-mercaptoethanol (BME). Like DTT, BME is a reducing agent that prevents crosslinking. An elution buffer was also prepared with 500 mM imidazole and 2 mM BME dissolved in PBS, vacuum filtered and pH=7.4.

Three SNAP-25-TS purifications were performed using this Ni-NTA column, one for each buffering condition (5 mM, 10 mM, and 20 mM imidazole in the equilibration buffer). The pellet of SNAP-25 TS containing cells was resuspended in 10 ml of equilibration buffer and sonicated at 12 Watts using the probe sonicator for five minutes. The solution was then centrifuged at 14,000 rpm for 25 minutes at 4°C to remove the cell debris. The supernatant was subsequently

www.manaraa.com

passed through a 0.45 μm filter and was then added to the Ni-NTA column in 1 ml fractions. The column was then washed 15 times with equilibration buffer to remove any proteins nonspecifically bound to the column. After the 15th wash step, the elution buffer was added in 1 ml fractions, and each of these elution fractions was collected in Eppendorf tubes. Ten elution fractions total were collected for each purification.

After testing 5 mM, 10 mM, and 20 mM concentrations of imidazole in the equilibration buffer, the 20 mM imidazole buffering condition was found to be best at minimizing nonspecific binding, as revealed by SDS-PAGE. Figure 2.7 shows the 10% SDS-PAGE gels comparing the SNAP-25 T-Sapphire purifications using varying concentrations of imidazole in the equilibration buffer. The first elution fraction is shown for 5 mM, 10 mM, and 20 mM imidazole purifications. As the concentration of imidazole increases, the number of protein bands in the elution fraction decreases, which is indicative of fewer protein contaminants.

www.manaraa.com

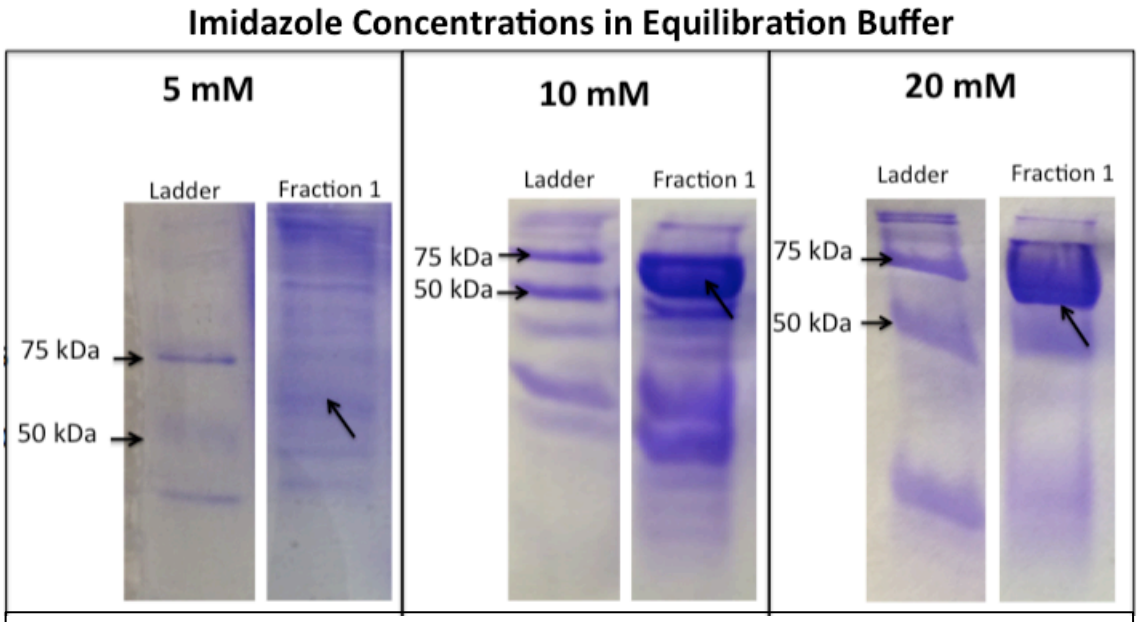

Figure 2.7 10% SDS-PAGE gels comparing the various imidazole concentrations in the equilibration buffer during purification on a 5 ml column packed with Ni-NTA beads. The first panel shows a purification using 5 mM imidazole in the equilibration buffer, the second panel is a purification with 10 mM imidazole, and the third panel is a purification with 20 mM imidazole. The first elution fraction is shown for each purification. The arrow points to the SNAP-25 T-Sapphire bind (~64.2 kDa). As the concentration of imidazole in the equilibration buffer increases, the number of protein bands in the elution fraction decreases, which indicates fewer contaminants and a more pure sample.

www.manaraa.com

2.3.4 **Purification on the FPLC**

Once buffering conditions were optimized, the SNAP-25 T-Sapphire was purified on the FPLC. The frozen cell pellet was thawed in a water bath at room temperature. Using a glass rod, the cells were resuspended in 20 ml of equilibration buffer (20 mM imidazole and 2 mM BME dissolved in PBS and vacuum filtered, pH=7.4). One protease inhibitor tablet (Roche) was dissolved in the solution before 10 rounds of sonication on the probe sonicator for 30-second intervals at 12 Watts. Once the cells were sufficiently lysed, the solution was centrifuged at 14,000 rpm for 30 minutes at 4°C. The cell debris was discarded, and the supernatant was loaded into the HisTrap FF column (GE) on the FPLC. A linear gradient of imidazole from 20 mM to 500 mM was flowed through the column to elute off the protein, and fractions that corresponded to a high UV signal were collected. These fractions were also viewed under UV light to confirm fluorescence (Figure 2.8).

Purity was assessed by running a 10% SDS-PAGE protein gel (Figure 2.9). In an attempt to further concentrate and purify the protein, two rounds of dialysis were performed in thiol buffer (20 mM citric acid, 35 mM Na_2HPO_4, 108 mM NaCl, and 1 mM EDTA, pH=6.5) at 4°C. This buffer was chosen because it has been shown to stabilize vesicles, and citric acid, as an electron donor, is a reducing agent. The slightly acidic pH of the buffer also helps to keep the protein reduced and prevents crosslinking [22].

www.manaraa.com

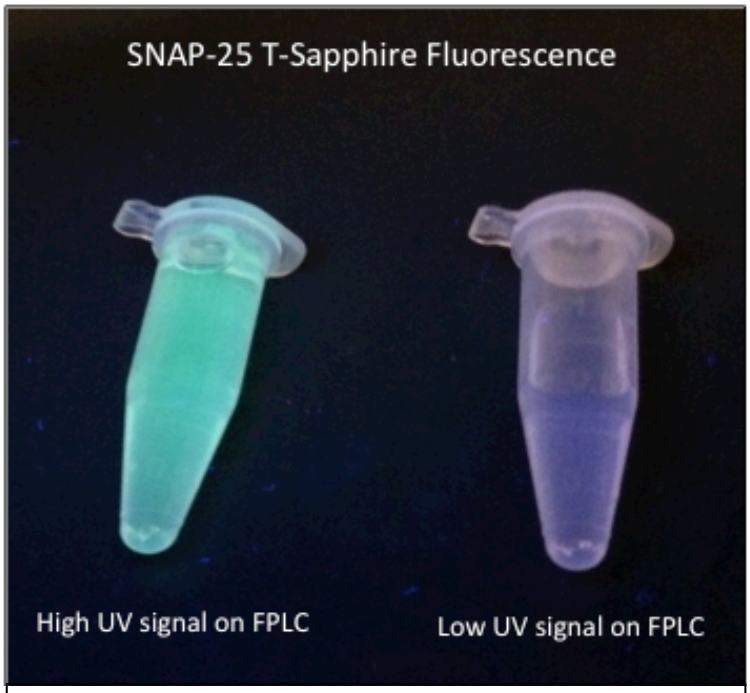

Figure 2.8 Sample fractions taken from the FPLC purification of SNAP-25 T-Sapphire and imaged under UV light. The elution fraction on the left contains the fluorescent protein and corresponds to a high UV signal on the FPLC, while the fraction on the right is not fluorescent and had a low UV signal on the FPLC.

www.manaraa.com

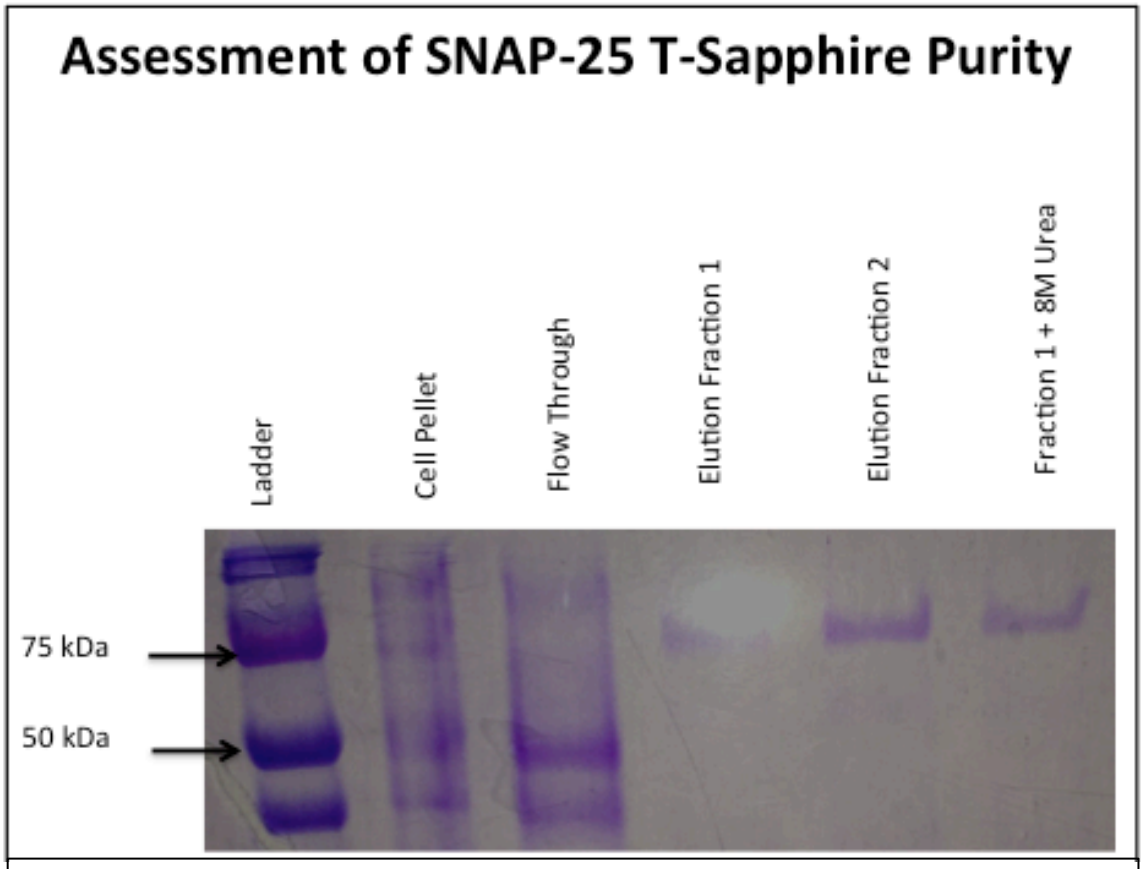

Figure 2.9 10% SDS-PAGE gel assessing the purity of SNAP-25 T-Sapphire after purification on the FPLC. SNAP-25 T-Sapphire is 64.2 kDa. Elution fractions 1 and 2 were fluorescent and had a high UV signal on the FPLC. In the last lane of the gel, 8M urea was added to Elution Fraction 1 before running the gel to ensure that the protein is not aggregating and is in its monomeric form.

www.manaraa.com

2.3.5 **Discussion**

Initial attempts at purifying SNAP-25 T-Sapphire provide promising results. The emission peak at 511 nm seen 24 hours after induction (Figure 2.6) indicates that the T-Sapphire protein is being expressed and is fluorescent. Additionally, the fact that distinct elution fractions with a relatively high UV signal were generated during the FPLC purification and that these fractions were fluorescent (Figure 2.8) further illustrates that the purification worked correctly. The 10% SDS-PAGE gel in Figure 2.9 confirms that the SNAP-25 T-Sapphire protein is present and relatively pure, although a few faint bands can be seen underneath the SNAP-25 TS band. Furthermore, the addition of 8M urea to the purified SNAP-25 TS reveals that the protein is in its reduced (monomeric) form and has not aggregated. At a concentration of 8M, urea is a strong denaturant, so if the protein were dimerizing, it would have been revealed in the gel.

In an attempt to remove any remaining impurities from the SNAP-25 TS, dialysis was performed after purification on the FPLC. Dialysis was performed as previously described (Section 2.2.3). Unfortunately, in these preliminary experiments, inefficiencies in the dialysis process led to the loss of protein, so the remaining concentration was extremely low at 200 nM (measured on the Nanodrop). Figure 2.10 shows a 10% SDS-PAGE gel of the SNAP-25 TS protein after dialysis. As the protein is of relatively high purity before dialysis, in future purifications, the dialysis can probably be omitted with no major consequences. Despite the low concentration of the protein after dialysis, we were still able to

www.manaraa.com

demonstrate binding of the SNAP-25 T-Sapphire construct to lipid-coated microspheres. These results are presented in Chapter 4.

www.manaraa.com

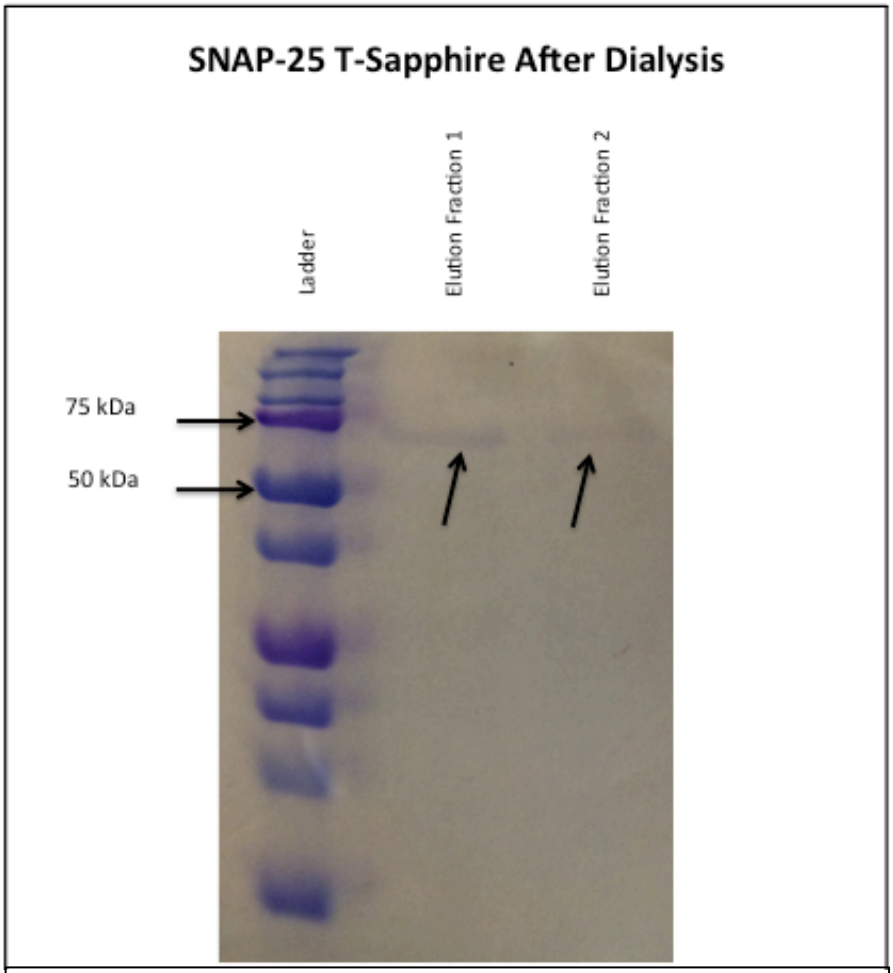

Figure 2.10 10% SDS-PAGE gel depicting the purified SNAP-25 TS protein after two rounds of dialysis. The arrows point to the protein band for SNAP-25 TS (64.2 kDa).

www.manaraa.com

2.4 Chapter Summary and Conclusions

Chapter 2 describes the construct design and purification of SNAP-25 GFP, as well as the brand new protein construct, SNAP-25 T-Sapphire. The TS fluorophore is a GFP mutant and is more stable and has improved folding compared to GFP, as well as a significantly larger Stokes Shift [20]. For these reasons, efforts are underway to switch fluorescence-based SNAP-25 protease assays to this new T-Sapphire chromophore. The T-Sapphire plasmid was synthesized by GenScript, and a restriction digestion was performed to ensure plasmid correctness. Fluorescence measurements after induction confirm that the protein is being induced and expressed. Buffering conditions for the purification were optimized, and SDS-PAGE reveals that we were able to purify the protein in these initial FPLC protocols. However, impurities in the protein still exist, and dialysis and filtration methods after purification must be optimized further. Ultimately, however, both GFP and T-Sapphire SNAP-25 protein were successfully obtained, allowing for the performance of the measurements presented in the remainder of this thesis.

Chapter 3

ASSAY DESIGN AND ATTACHMENT OF SNAP-25 TO MICROSPHERES

3.1 Introduction

Supported lipid bilayers (SLBs) on microspheres are used for a variety of biomedical applications due to their ability to mimic a biological membrane [23]. SLBs are composed of a phospholipid bilayer where the hydrophobic tail groups

www.manaraa.com

of the lipids are oriented inwards, and the hydrophilic head groups are oriented outwards. While greatly oversimplified compared to a eukaryotic membrane, SLBs still have many advantages in their ability to mimic a biological environment [23]. First, due to the fact that a very thin (1-2 nm) layer of water sits between the microsphere and the membrane, SLBs are able to maintain lateral fluidity comparable to a biological membrane [23]. Figure 3.1 shows the structure of a SLB on a silica microsphere. Additionally, these silica microspheres provide a stable platform for the study of membrane proteins once they are inserted into the bilayer [23]. Soluble proteins can be anchored to the lipid bilayer using a variety of attachment strategies [23]. In the present context, we hypothesize that the membrane plays a key role in facilitating the interactions between proteases and membrane-bound substrates. Therefore, we hope to study these interactions in the presence of a membrane in order to gain a more complete understanding of the enzymatic processes involved in proteolytic cleavage, and for such studies, the use of SLBs formed on microspheres is an excellent material platform.

www.manaraa.com

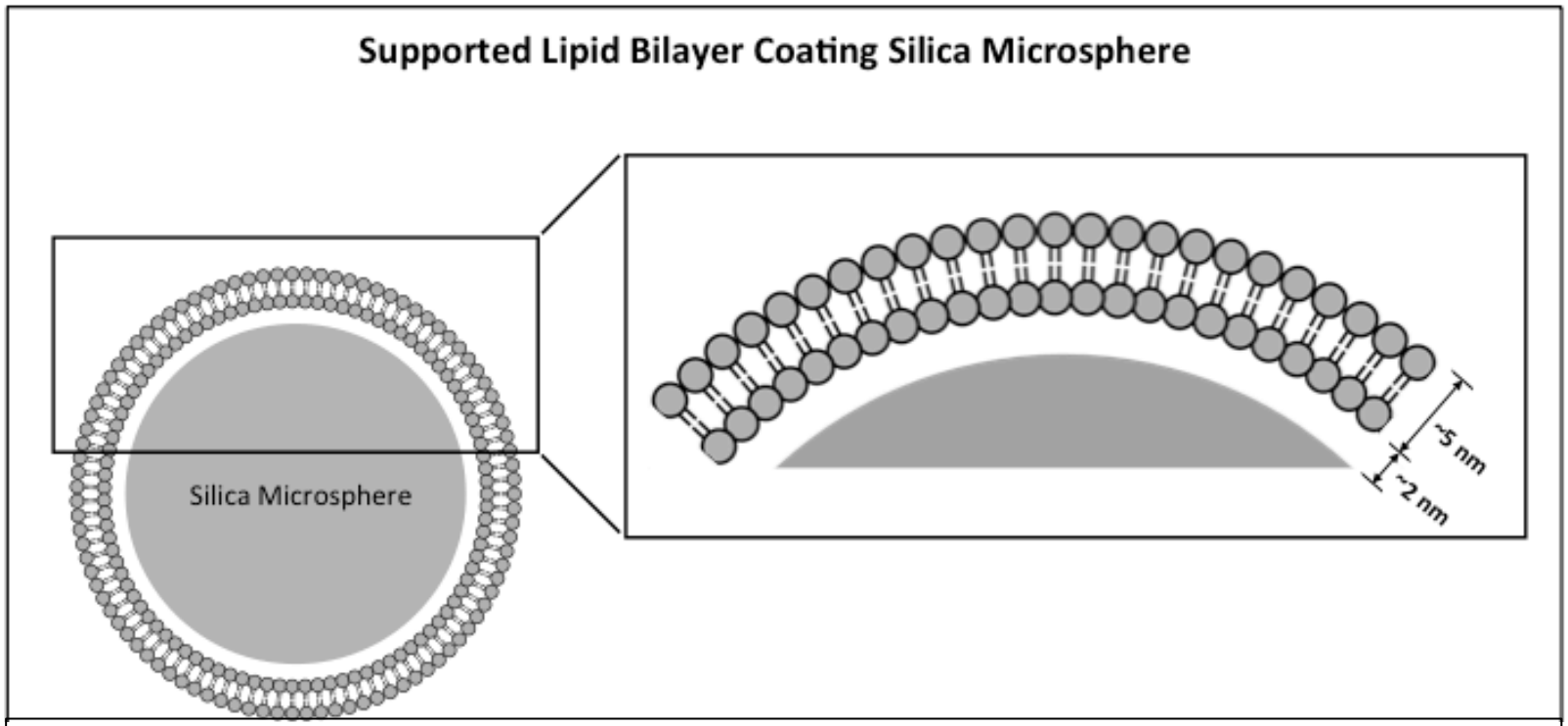

Figure 3.1 Illustration of a supported lipid bilayer formed around a silica microsphere. A thin, 2 nm layer of water separates the microsphere from the phospholipid bilayer, thus mimicking the lateral mobility of a biological membrane. Figure adapted from Chemburu, S. *et al.* (2010). [23]

www.manaraa.com

3.2 Attachment Strategy of SNAP-25 to Lipid-Coated Microspheres

In order to peripherally attach SNAP-25 to a membrane-coated microsphere, we employed sulfhydryl-reactive crosslinking. Sulfhydryls (thiols) are one of the most common crosslinkers used in bioconjugation techniques, second only to primary amines [24]. We chose to use thiol crosslinking for several reasons. First, due to the fact that sulfhydryls are present in most proteins but are not as common as primary amines, the amount of crosslinking can be more precisely controlled [24]. Second, because sulfhydryls in proteins generally form disulfide bonds, crosslinking at these regions rarely blocks binding sites or alters native protein structure [24].

The side chains of cysteine residues in SNAP-25 contain sulfhydryls (--SH), and pairs of these sulfhydryl groups are generally linked by a disulfide bond within the protein (--S-S--). When in the reduced form (--S), they are free to bind with thiol-reactive compounds [24]. Maleimides specifically react with sulfhydryls by forming a stable and irreversible thioether linkage when conjugated between pH 6.5 and 7.5 (mechanism shown in Figure 3.2) [24]. Using this attachment chemistry, we can reduce the SNAP-25 protein so that its sulfhydryl groups are free to form a disulfide bridge with the maleimide-containing lipid, 1,2-dihexadecanoyl-*sn*-glycero-3- phosphoethanolamine-N- [4-(p-maleimidophenyl)butyramide] (MPB-PE). We coat nonporous silica microspheres with lipid bilayers that contain various concentrations of this MPB-PE lipid, which can then form a disulfide bond with the sulfhydryls in the SNAP-25 protein. This attachment strategy gives us the ability to study

www.manaraa.com

protease/substrate interactions in the presence of a lipid membrane. A schematic of this sulfhydryl attachment is shown in Figure 3.3.

www.manaraa.com

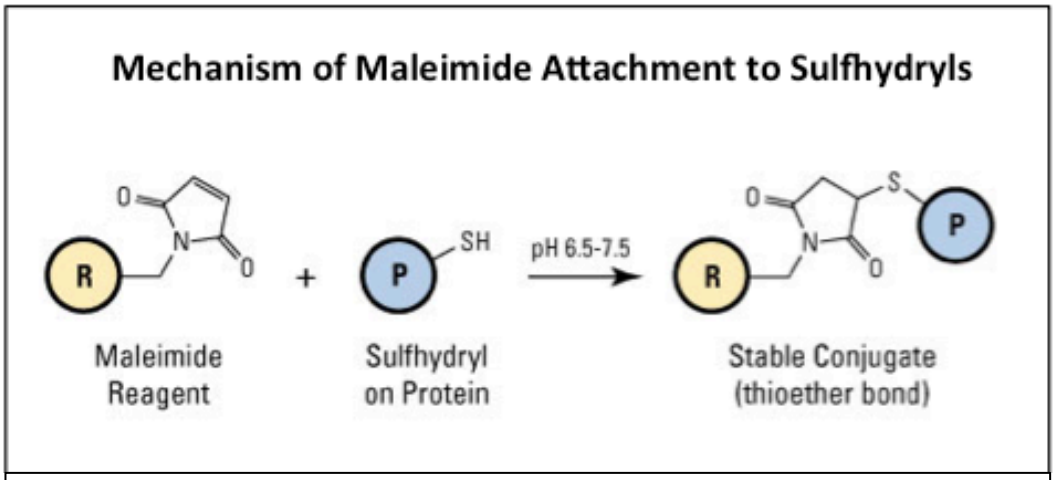

Figure 3.2 Mechanism of protein conjugation with a maleimide group. Figure taken from *Bioconjugate Techniques, 3rd Ed.* [24].

www.manaraa.com

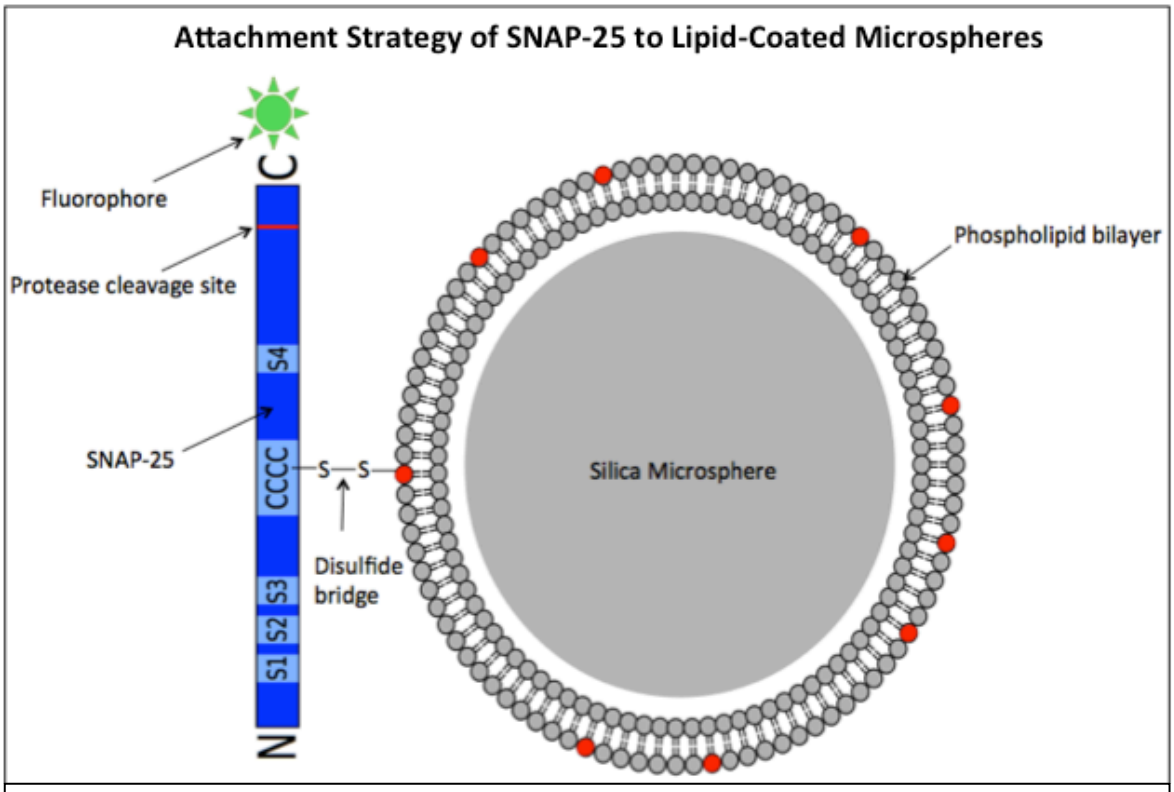

Figure 3.3 Attachment strategy of fluorescently-tagged SNAP-25 to a lipid-coated microsphere. The SNAP-25 protein is shown in blue, with a fluorescent molecule (green) attached at the C terminus. The maleimide-containing lipid MPB-PE is shown in red and can form a disulfide bridge with the cysteine residues on the SNAP-25. Figure adapted from José Cornejo's thesis [30].

www.manaraa.com

3.3 Materials and Methods

3.3.1 Lipid Preparation

1 mM stock solutions were prepared of the following lipids in chloroform: 1-palmitoyl-2-oleoyl-sn-glycero-3-phosphocholine (POPC) and 1,2-dihexadecanoyl-*sn*-glycero-3-phosphoethanolamine-N-[4-(p-maleimidophenyl) butyramide] (MPB-PE). From these stock solutions, chloroform solutions with the following mole percentages were prepared in glass vials, typically with a total lipid concentration of 1 mM in 800 µl volume: 1) 100% POPC 2) 99% POPC and 1% MPB-PE 3) 95% POPC and 5% MPB-PE 4) 90% POPC and10% MPB-PE. Figure 3.4 shows the structure of the two lipids used in this study and discusses some of their key properties. The vials were left under vacuum overnight to evaporate off the chloroform, and then the lipid film was rehydrated in thiol buffer (20 mM citric acid, 35 mM Na_2HPO_4, 108 mM NaCl, and 1 mM EDTA, pH=6.5) to a final lipid concentration of 1 mM (again, typically at 800 µl total volume). After adding buffer, the samples were vortexed by hand until the lipids were resuspended in solution. In order to create monodispersed liposomes, the samples were passed through an Avanti extruder (0.1 µm membrane) at least 17 times (or, if necessary, until the solution turned from cloudy to clear). This solution was then aliquoted into autoclaved Eppendorf tubes at a sample volume of 250 µl each.

www.manaraa.com

Structure and Key Properties of POPC and MPB-PE Lipids

18:1 MPB-PE

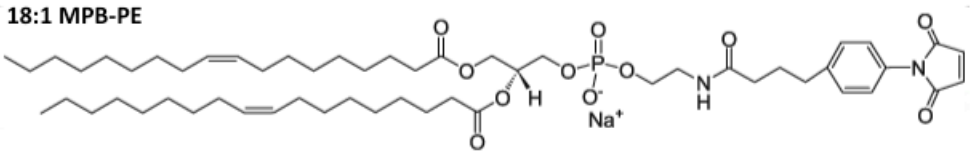

16:0 – 18:1 POPC

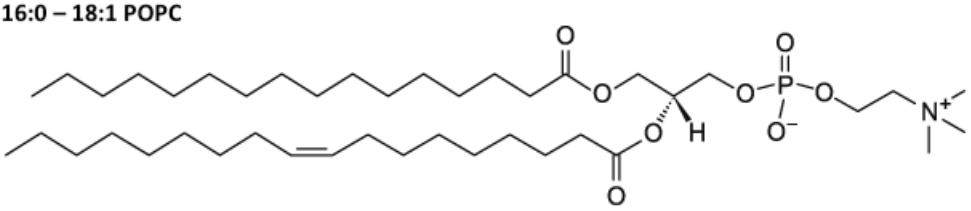

Lipid	Molecular Formula	MW (g/mol)	Transition Temperature (°C)
MPB-PE	$C_{55}H_{88}N_2O_{11}PNa$	1007.2	-16 (estimated from DOPE)
POPC	$C_{42}H_{82}NO_8P$	760.1	-2

Figure 3.4 Structures and properties of the phospholipid POPC and maleimide-containing lipid MPB-PE. Images taken from Avanti [31].

www.manaraa.com

3.3.2 Characterization of Microspheres using Flow Cytometry

Three micron, nonporous silica microspheres (Spherotech) were chosen for this study for several reasons. First, these microspheres are roughly similar in size to eukaryotic cells (~10 microns) or organelles (~1 micron), and in an effort to make these particles biomimetic, we try to mimic structures of mammalian cells as closely as possible. Second, the fact that these beads are nonporous is advantageous because the absence of pores on the bead surface can help ensure a more even lipid coating, and a bulk silica surface is generally better characterized and understood than porous surfaces. Third, a large body of literature exists that use supported lipid bilayers on silica microspheres [23,25,26], so we can draw from this previous work.

In order to determine the optimal number density of beads to use, we performed a series of serial dilutions from ~10^8 to ~10^4 beads/ml and counted the particles on the Accuri flow cytometer. We found that the ability for the Accuri to reliably count individual particles saturates at a particle concentration of approximately 7×10^6 beads/ml (Figure 3.5). Based on this data, we determined that a good choice for number density of beads to use is well below this saturation point, or approximately 10^6 beads/ml.

www.manaraa.com

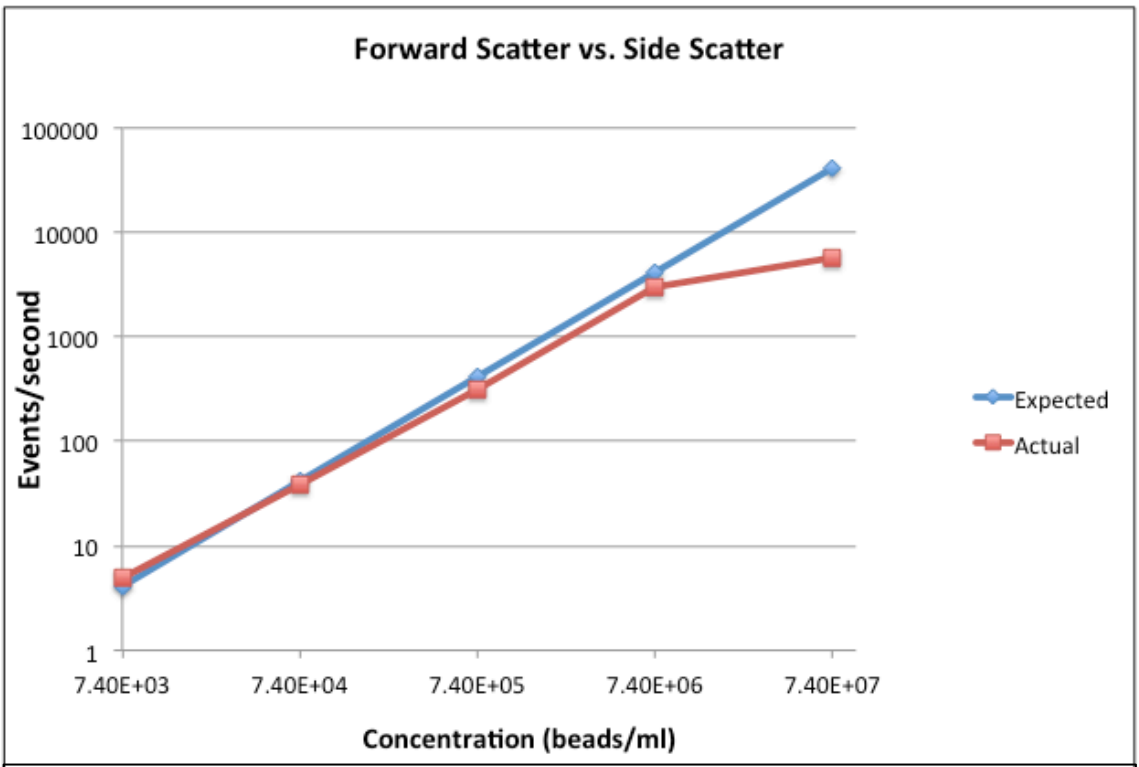

Figure 3.5 Particle counting experiment on the Accuri flow cytometer using 3 micron nonporous silica beads. The blue line depicts expected events/second, which were calculated by multiplying the flow rate (ml/min) by the concentration (beads/ml), and converting to second. The red line depicts the actual number of events/second.

www.manaraa.com

After determining the optimal number of beads to add to the lipids, we wanted to ensure that we have enough lipids per sample to sufficiently coat this volume of beads. In other words, the lipids must be in great excess of the beads. The following estimate was performed:

***Surface Area of a Sphere**:* $A=4\pi r^2$

From the Spherotech data sheet, the mean silica bead diameter is 3.14 μm (r=1.57 μm)

$A=4\pi\ (1.57\ \mu m)^2 = 30.97\ \mu m^2$/ bead

Area of POPC Head Group= 70Å^2 per lipid = $7*10^{-7}$ μm^2/lipid

Determining Lipids per Bead:

$$\frac{30.97\ \frac{\mu m^2}{bead}}{7 * 10^{-7}\ \frac{\mu m^2}{lipid}} = \frac{4.42 * 10^7\ lipids}{bead} \quad \textbf{(monolayer)}$$

$$\frac{4.42 * 10^7\ lipids}{bead} \times 2 = \frac{8.85 * 10^7\ lipids}{bead} \quad \textbf{(bilayer)}$$

Determining Number of Lipids per mL:

$$\frac{8.85 * 10^7 lipids}{bead} \times \frac{10^6 beads}{mL} = \frac{8.85 * 10^{13} lipids}{mL}$$

Determining Number of Lipids Required to Coat Beads in a 250 µl Sample of 1 mM Lipid Solution:

$$\frac{8.85 * 10^{13}\ \text{lipids}}{mL} * 0.250\ \text{mL} = 2.21 * 10^{13}\ lipids$$

Determining Total Number of 1 mM Lipids in 250 µl Sample:

$$\frac{0.001\ mol}{L} * \frac{6.02 * 10^{23}\ lipid\ molecules}{mol} * 0.00025\ L = 1.51 * 10^{17} lipids$$

www.manaraa.com

Determining Lipid Excess:

$$\frac{1.51 * 10^{17}\ lipids\ in\ sample}{2.21 * 10^{13}\ lipids\ required} = 6.83 * 10^{3}\ \ lipid\ excess$$

This calculation shows that the available lipids are in approximately 7,000-fold excess of the lipids required for full bead coverage.

3.3.3 Formation of Lipid Bilayers around Microspheres

After determining the optimal number of beads to add to the lipid solution, we can form supported lipid bilayers (SLBs) around the microspheres. Beads were added to each of the following samples at a concentration of 10^6 particles/ml: 100% POPC + 0% MPB-PE, 99% POPC + 1% MPB-PE, 95% POPC + 5% MPB-PE, and 90% POPC + 10% MPB-PE. The samples were then placed in a vortex carousel (VWR) on high at room temperature for ten minutes, and then vortexed on low speed for 45 minutes at 37°C. The SLBs form spontaneously around the microspheres. In order to confirm that the beads are adequately coated with lipids, 0.5 molar percent of a headgroup-labeled carboxyfluorescein lipid, 1,2-dioleoyl-sn-glycero-3-phosphoethanolamine-N-carboxyfluorescein (CF-PE), was integrated into the membrane for imaging on a confocal microscope (Zeiss) and subsequent analysis on the Accuri flow cytometer. In confocal microscopy, Z-stack slices were taken in 1 micron slices through the microspheres to further verify the presence of an even and complete lipid coating. Figure 3.6 shows confocal images of lipid-coated beads at various maleimide lipid concentrations as well as the median fluorescence values and

www.manaraa.com

flow cytometry data from the corresponding samples, as measured on the Accuri C6.

www.manaraa.com

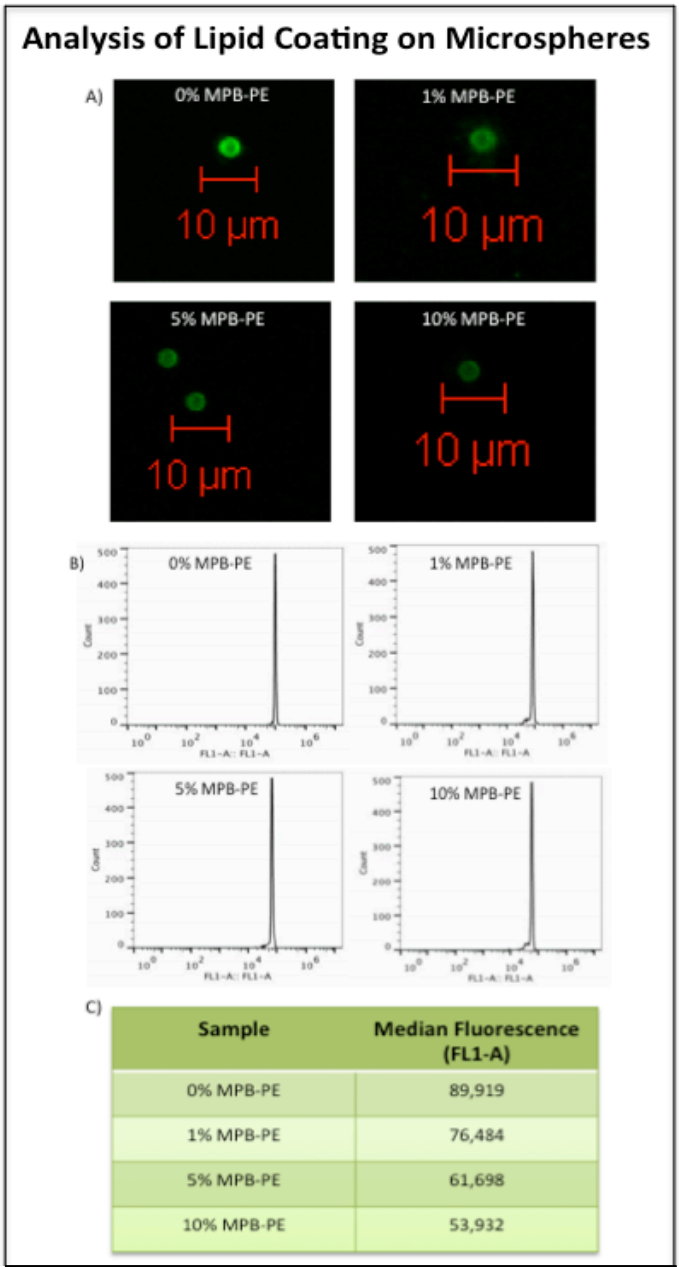

Sample	Median Fluorescence (FL1-A)
0% MPB-PE	89,919
1% MPB-PE	76,484
5% MPB-PE	61,698
10% MPB-PE	53,932

Figure 3.6 Analysis of lipid coating on silica microspheres. A) Confocal images taken of samples with 0%, 1%, 5%, and 10% MPB-PE. The remainder of the bilayer is composed of POPC and 0.5% CF-PE. Images were taken on the Zeiss confocal microscope with a 63X oil immersion lens. B) Flow cytometric data corresponding to the samples imaged on the confocal. Measurements were taken on the Accuri C6 flow cytometer. C) Median fluorescence values corresponding to the histograms in B.

www.manaraa.com

3.3.4 Bovine Serum Albumin (BSA) Blocking

A BSA block was incorporated into the protocol for several reasons. First, as mentioned previously, impurities in the SNAP-25 GFP can lead to nonspecific binding of protein contaminants to the lipid membrane. Second, BSA can block portions of the silica surface that are exposed due to defects in the membrane. It has been shown in the literature that 100 μg/ml of BSA is the optimal concentration for preventing nonspecific binding on SLBs because nonspecific interactions are sufficiently blocked at this concentration while still maintaining the lateral mobility and structural integrity of the membrane [27]. Blocking with higher concentrations of BSA can lead to holes in the bilayer where the BSA has displaced portions of the membrane, and lower concentrations do not adequately prevent nonspecific binding [27]. Based on these results, 100 μg/ml of BSA were added to each sample and allowed to incubate on the shaker at low speed at room temperature for 45 minutes. In order to remove any unbound BSA in solution, three wash steps were performed by centrifuging the samples at 10,000 rpm for 45 seconds, removing the supernatant (being careful to leave the bead pellet hydrated), and resuspending the beads in fresh buffer. After the last wash step, the beads were resuspended in 100 μl of buffer instead of 250 μl in order to leave room for the addition of SNAP-25 GFP. After the BSA blocking and wash steps are completed, the SNAP-25 protein can be conjugated to the maleimide lipids in the membrane. Figure 3.7 compares SNAP-25 GFP binding in samples that were blocked with BSA versus no blocking. The x-axis represents fluorescence intensity, while the y-axis shows event count. The red lines depicts samples where

www.manaraa.com

no SNAP-25 GFP was added, the blue lines are samples with 200 nM SNAP-25 GFP, and the orange lines are samples with 500 nM SNAP-25 GFP. Both data sets shown in this figure were prepared using 100% POPC for the lipid coating and do not contain any MPB-PE. Because there are no maleimide-containing lipids for the SNAP-25 GFP to bind to, the fluorescence intensity should not depend on SNAP-25 GFP concentration. In the graph on the left with no BSA blocking, however, the fluorescence intensity increases as the concentration of SNAP-25 GFP increases, indicating that the protein is nonspecifically binding to the microsphere. In contrast, in the graph on the right where a BSA block was performed, the fluorescence intensity does not change with increasing concentrations of SNAP-25 GFP, indicating that the BSA is effectively blocking the protein from nonspecifically binding to the microsphere.

www.manaraa.com

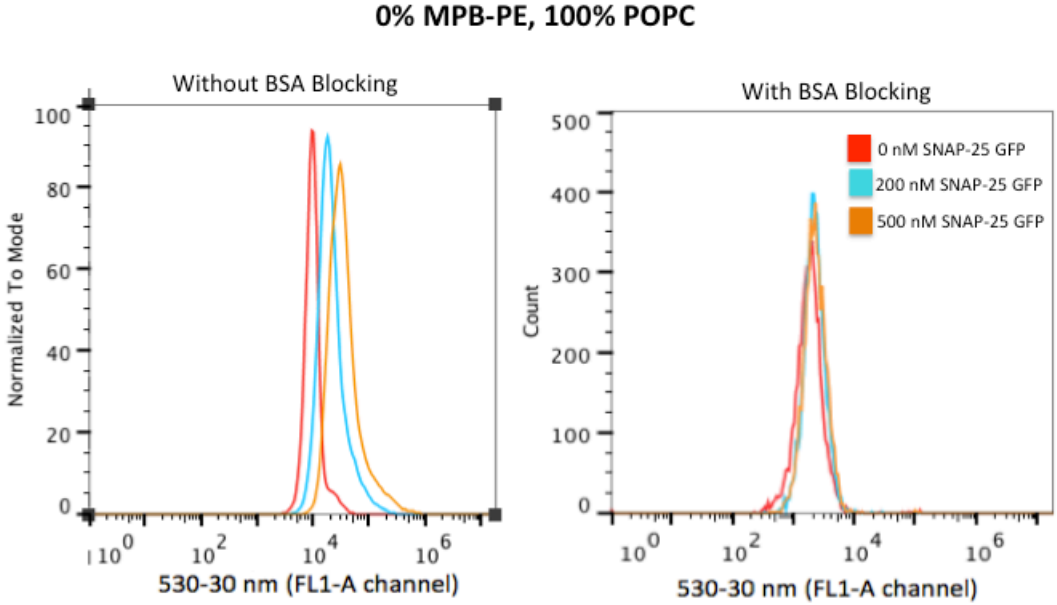

Figure 3.7 Comparison of SNAP-25 GFP conjugation to lipid-coated microspheres with and without BSA blocking. The membranes coating these microspheres contain no MPB-PE and are 100% POPC. The red line depicts samples with no SNAP-25 GFP added, the blue line depicts samples with 200 nM SNAP-25 GFP, and the orange line are samples with 500 nM of SNAP-25 GFP.

www.manaraa.com

3.3.5 Conjugation of SNAP-25 to MPB-PE

Because the reducing agent DTT was incorporated into the equilibration and elution buffers during purification, the SNAP-25 GFP should already be in its reduced form. This is confirmed using SDS-PAGE by the absence of a protein dimer band (Figure 2.3). Residual DTT was removed from the sample by centrifugation with a MWCO filter and dialysis (described previously in Chapter 2). Buffer and then SNAP-25 GFP (at concentrations of 0 nM, 200 nM, and 500 nM) were added to samples to bring the sample volume back up to 250 µl. To prevent oxidation of the protein, all samples were passed under an argon stream for 30 seconds. They were then placed on a rotator overnight at 4°C to allow time for the SNAP-25 GFP to bind to the MPB-PE. Results that confirm SNAP-25 GFP binding to lipid-coated microspheres are shown in Figure 3.8. In this figure, fluorescence intensity is shown on the x-axis and event count is shown on the y-axis. In the histogram to the left, the membrane contains 100% POPC and no maleimide-containing lipid MPB-PE. 0 nM of SNAP-25 GFP is shown in red, 200 nM is in blue, and 500 nM is in orange. The fact that the peaks strongly overlap indicates that there is little nonspecific binding occurring. In the graph on the right, the following concentrations of SNAP-25 were added to microspheres coated with a membrane containing 10% MPB-PE + 90% POPC lipids: 0 nM SNAP-25 GFP in red, 200 nM in blue, and 500 nM in orange. We would expect the fluorescence intensity to increase as the concentration of fluorescent protein increases, and this trend is clearly visible.

www.manaraa.com

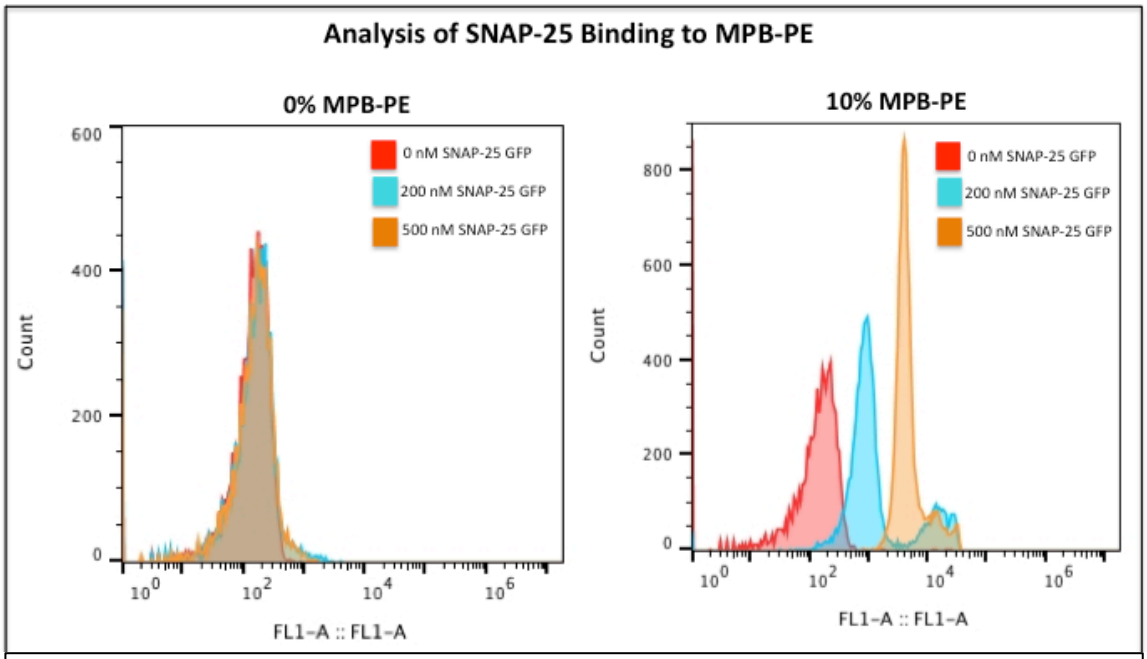

Figure 3.8 Analysis of SNAP-25 GFP binding to lipid-coated microspheres. The graph on the left is 100% POPC and contains no maleimide lipid, and the graph on the right contains 10% MPB-PE + 90% POPC. The red line represents samples with 0 nM SNAP-25 GFP, the blue line is 200 nM SNAP-25 GFP, and the orange line is 500 nM SNAP-25 GFP.

www.manaraa.com

3.3.6 **Incubation with Protease**

After confirmation that the SNAP-25 GFP is sufficiently binding the lipid membrane, proteases were introduced to the samples. All samples were split into thirds (one control set where no protease was added, one set where trypsin was added, and one set where BoNT/A was added). Figure 3.9 outlines the sample preparation and analysis for this portion of the study.

Trypsin is a protease that catalyzes the hydrolysis of peptide bonds at the C-terminal side of lysine and arginine amino acids [28]. Because virtually all proteins contain these residues, trypsin is often used as a general protease [28]. We employ trypsin as a positive control to show that proteolytic cleavage of SNAP-25 GFP is occurring. BoNT/A, on the other hand, has an extremely high specificity for SNAP-25, so proteolytic cleavage of SNAP-25 by BoNT/A will not only allow for detection of the toxin, but will also provide important information regarding the enzymatic activity of the toxin's interaction with its membrane-bound substrate. After the proteases are added, the samples are placed on a rotator at 37°C to incubate.

www.manaraa.com

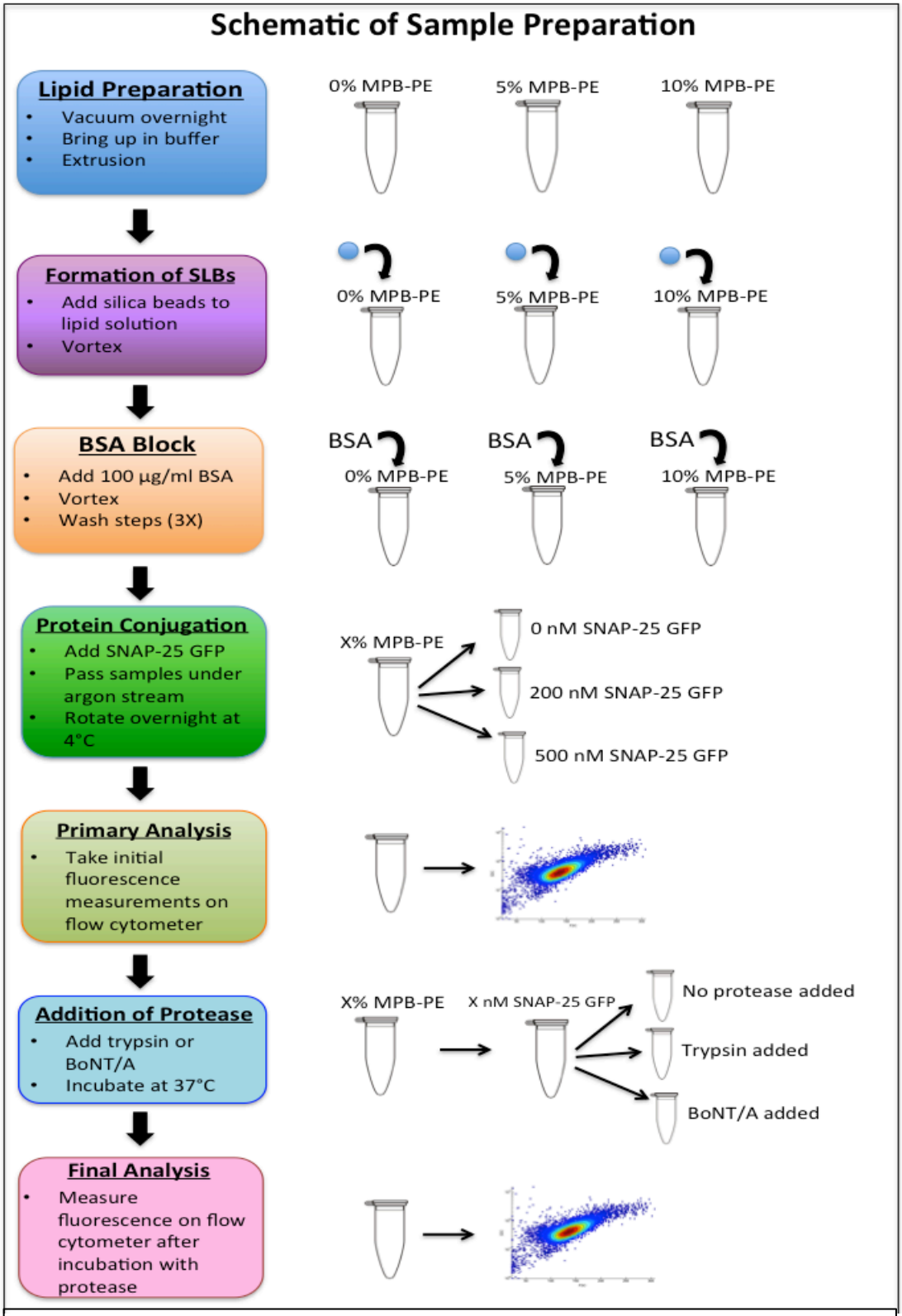

Figure 3.9 Schematic depicting the steps of sample preparation and analysis of SNAP-25 GFP conjugation to membrane-coated microspheres and subsequent proteolytic cleavage.

www.manaraa.com

3.3.7 Flow Cytometric Analysis

Initial measurements are taken on the Accuri C6 flow cytometer after the overnight conjugation of SNAP-25 GFP to the lipid-coated microspheres. The samples are measured again immediately after addition of the protease, and then every hour after addition for two hours. This allows us to correlate protease activity with time. The results of these protease cleavage assays are shown in Section 3.4.

3.4 Results

Three replicates of the Trypsin/BoNT protease assay were preformed. The samples that exhibited the best binding of the SNAP-25 GFP to the lipid membrane were samples with 10% MPB-PE and 500 nM of protein, so the data analysis presented in the remainder of this section reflects samples prepared under these conditions. A discussion of how to improve upon the current protein conjugation protocol can be found under Future Directions (Section 4.2).

Figure 3.10 exhibits the results of the three individual Trypsin/BoNT protease assays. The x-axis shows the control, trypsin, and BoNT/A samples for each of the three replicates, and the y-axis represents median fluorescence intensity, as measured on the Accuri C6 flow cytometer. The blue lines are the samples before the addition of the protease, the red lines are measurements taken shortly after the protease was added (approximately 10 minutes), the green lines are 1 hour after protease addition, and the purple lines are after 2 hours incubation with the protease. The median fluorescence values were then averaged and

www.manaraa.com

plotted, and the standard deviation was used to make error bars. This data is shown in Figure 3.11. Next, the averages of the three replicates for 10% MPB-PE, 500 nM SNAP-25 GFP were plotted, and the median fluorescence was normalized to the control samples (no protease added) at each time point. These results can be seen in Figure 3.12. In this graph, the x-axis represents time (hours), where t=0 is just before addition of the protease. The y-axis is the ratio of the median fluorescence to that of the control sample at each time point. Trypsin is seen in blue, and BoNT/A is seen in red. Finally, a histogram that shows the loss of fluorescence over time after incubation with the BoNT/A toxin for a single replicate is also presented in Figure 3.13.

www.manaraa.com

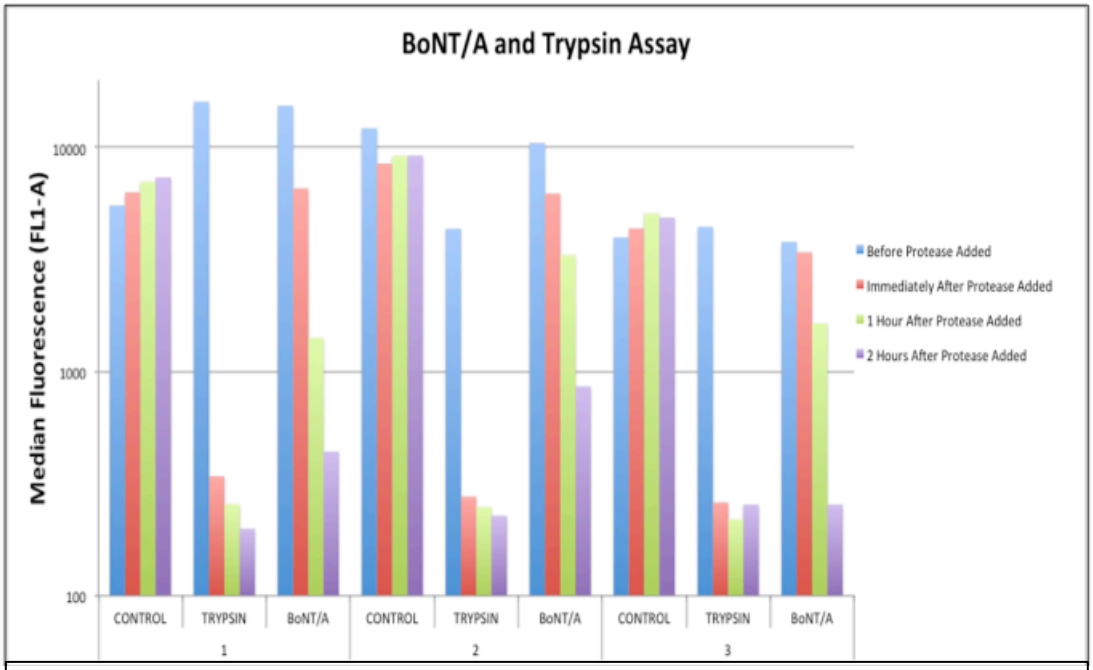

Figure 3.10 Results of three separate experiments after incubation with the Trypsin of BoNT/A LC proteases. Median fluorescence is seen on the y-axis, and the sample is on the x-axis. The blue line represents samples before the protease was added, the red line is immediately after protease addition, the green line is after a 1 hour incubation with the protease, and the purple line is after 2 hours incubation.

www.manaraa.com

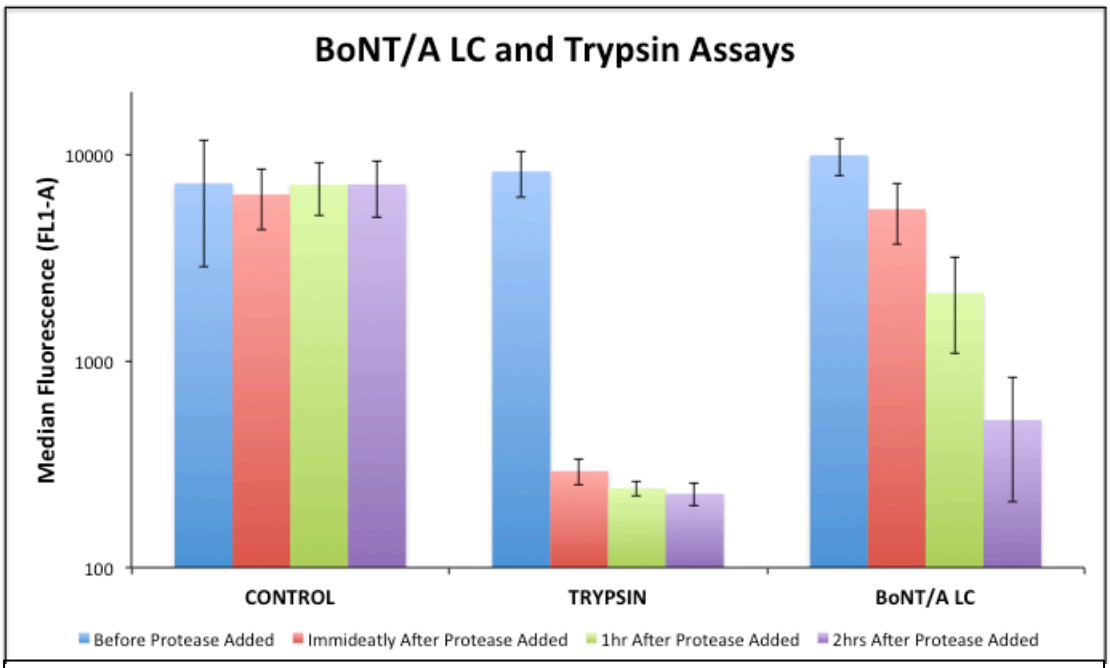

Figure 3.11 Results showing the average values of the three protease assay replicates. The error bars were plotted using the standard deviation. The x-axis represents the time points after addition of the protease for each sample, and the median fluorescence values are plotted on the y-axis. Time points before the protease was added are in blue, immediately after addition are in red, 1 hour after addition are in green, and two hours are in purple.

www.manaraa.com

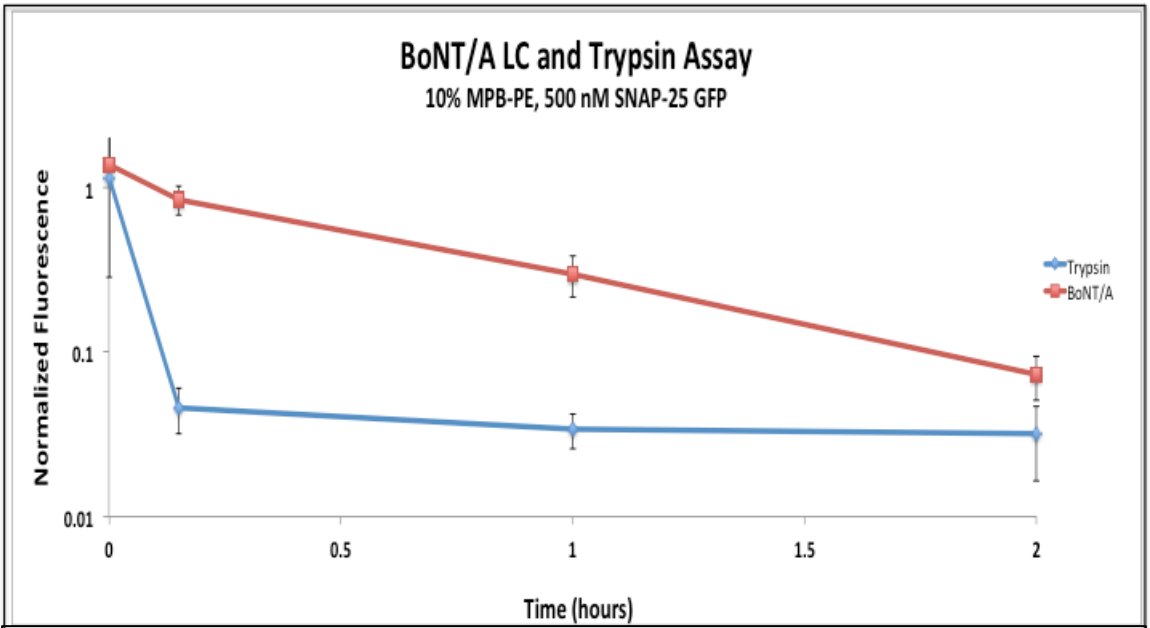

Figure 3.12 Graph depicting the activity of the BoNT/A LC and Trypsin proteases over time on samples with 10% MPB-PE lipid and 500 nM SNAP-25 GFP. Trypsin is seen in blue, and BoNT/A LC is red. The x-axis depicts time in hours. Time zero is before the protease was added, and time points were taken at 0.15, 1, and 2 hours after the protease was added. All median fluorescence values were normalized to the control samples (no protease added) at each time point, and the error bars were calculated using the standard deviation of these normalized fluorescence values.

www.manaraa.com

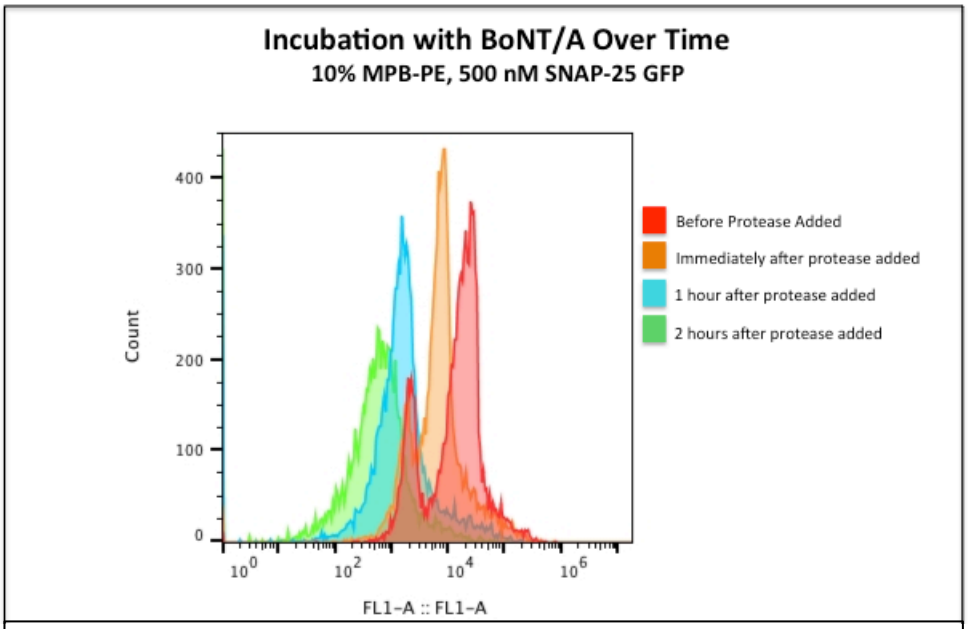

Figure 3.13 Histogram depicting flow cytometric data of 10% MPB-PE, 500 nM SNAP-25 GFP samples incubated with BoNT/A LC. Fluorescence intensity is on the x-axis, and count is on the y-axis. The red line depicts the samples before addition of the protease, the orange line is immediately after BoNT/A LC, the blue line is 1 hour after the protease was added, and the green line is 2 hours after addition. Loss of fluorescence can be observed over time.

www.manaraa.com

3.5 Discussion

The raw data of the three protease assay replicates plotted in Figure 3.10 clearly reveals a loss of fluorescence after incubation with the protease. The trypsin, as a positive control, works extremely quickly and takes the fluorescence to baseline within 10 minutes. The fluorescence decrease after adding the BoNT/A is slower, as expected, but the reaction seems to run to completion in all three cases after the two hour incubation period. While these results satisfy the overall objective of this project, it is clear that the process still needs to be optimized. In the first replicate, for example, the fluorescence of the trypsin and BoNT/A samples before addition of the protease are extremely high. Because no protease has been added at this point, the fluorescence values should be comparable to the control. There may have been some variation in the sample preparation. The third replicate exhibits the greatest amount of consistency of the fluorescence in both the control samples over time, and the control samples before addition of the protease.

In Figure 3.11, the same desired trend can be observed where the fluorescence intensity decreases over time after addition of the protease, with trypsin samples decreasing extremely quickly, and the BoNT/A samples running to completion after approximately 2 hours. Additionally, the error bars presented in this plot (by averaging all three replicates and calculating the standard deviation) probably over-estimate the error because while there is a great deal of variation between replicates, the numbers are much tighter within each individual experiment. The variation in fluorescence between replicates may be due to day-

www.manaraa.com

to-day variations in the Accuri C6 instrument, as well as variation in the sample preparation.

In Figure 3.12, all data was normalized to the control samples (no protease added) at each time point. While the greatest amount of error lies in the first time point (before the protease was added), the desired trend can still be seen where the trypsin causes loss of fluorescence very quickly, and the BoNT/A takes approximately two hours to run to completion.

Figure 3.13 demonstrates the loss of fluorescence after incubation with BoNT/A for a single sample (10% MPB-PE, 500 nM SNAP-25 GFP) over time. While the secondary peak is clearly visible in the control sample before the protease was added, the assay overall is achieving the desired effect.

3.6 Chapter Summary and Conclusions

In this chapter, we demonstrated specific binding of SNAP-25 GFP to a membrane-coated microsphere via attachment to the maleimide-containing lipid MPB-PE. BSA blocking procedures were optimized, and stability of the lipid coating surrounding these microspheres was assessed. We successfully demonstrated cleavage of the SNAP-25 GFP protein by both the trypsin and BoNT/A proteases and were able to quantify the enzymatic activity of these proteases on the protein substrate over time. While the need to optimize the protein binding and lipid preparation protocols still exist, we achieved the overall goal of this project to develop a flow-based assay for the study of proteases on membrane-associated substrates in the presence of a lipid bilayer.

www.manaraa.com

Chapter 4

SUMMARY AND FUTURE DIRECTIONS

4.1 Summary of Work

Poisoning by botulinum neurotoxins leads to the severe illness Botulism, which is characterized by flaccid paralysis, respiratory failure, and death. Due to the extreme toxicity of BoNTs, detection of the toxin is difficult, and current clinical diagnostic techniques take approximately 2-3 days to perform [1]. Furthermore, studies disagree on the mechanistic interpretations regarding the action of the toxin on its SNARE protein substrates [29]. In an effort to better understand the interaction between BoNTs and SNARE proteins in a psychologically relevant environment, we have developed a flow-based assay platform that allows for the study of BoNT activity in the presence of a membrane. The total assay time has been reduced to approximately 20 hours, and we can readily detect BoNTs in the nM range, which is comparable to many current techniques.

We have successfully purified two constructs of the SNAP-25 protein: SNAP-25 GFP and SNAP-25 T-Sapphire. We have demonstrated binding of the SNAP-25 GFP protein to the maleimide-containing lipid MPB-PE, thus anchoring the protein to a membrane-coated microsphere, enabling flow-based assays. We have also demonstrated that we can detect the presence of BoNT/A LC via flow cytometry by observing a loss of fluorescence after incubation with the protease.

www.manaraa.com

Again, due to the presence of a lipid bilayer, this system allows us to study how BoNTs act on membrane-bound proteins in a biological environment.

4.2 Future Directions

As described in Section 2.1, the T-Sapphire fluorophore has improved folding, is more stable under physiological conditions, and has a larger Stokes shift compared to GFP. In an effort to utilize these advantages, we must continue to optimize the expression and purification of the full-length SNAP-25 T-Sapphire construct. This effort is important in order to create a more robust system for the study of protease interactions with membrane-bound substrates. Figure 4.1 presents preliminary data showing the binding of purified SNAP-25 T-Sapphire to a lipid-coated microsphere containing 10% MPB-PE. This assay was prepared using the procedures described in Chapter 3 (the process is outlined in Figure 3.9). Measurements were taken on the LSR Fortessa flow cytometer with a 405 nm excitation wavelength. In this figure, the x-axis represents fluorescence intensity on a 525/50 nm channel, and the y-axis is event count. The sample with 0 nM SNAP-25 TS is seen in red, 50 nM SNAP-25 TS is in blue, and 100 nM is in orange. While there is not a great difference in binding between the 50 nM and 100 nM protein samples, there is a clear increase in fluorescence compared to the baseline (0 nM SNAP-25 TS) sample, indicating that the protein is binding to the maleimide-containing lipid MPB-PE in the membrane. While this preliminary data is encouraging, the SNAP-25 T-Sapphire purification and conjugation to lipid-coated microspheres must continue to be optimized.

www.manaraa.com

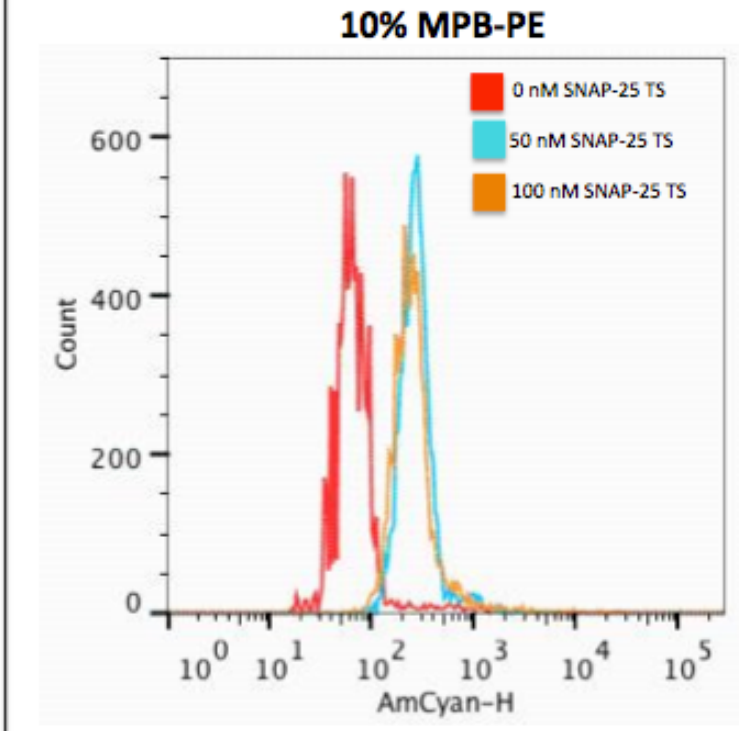

Figure 4.1 Preliminary data demonstrating the binding of SNAP-25 T-Sapphire to microspheres coated with 10% MPB-PE + 90% POPC lipids. The red line are samples with 0 nM SNAP-25 TS, the blue line is 50 nM SNAP-25 TS, and the orange line is 100 nM.

www.manaraa.com

In addition to optimizing the SNAP-25 T-Sapphire purification, the assay protocol must also be optimized in order to decrease nonspecific binding and increase stability of the lipid-coated microspheres. In many of the samples, a second fluorescent peak is visible after gating around the bead population in the flow cytometry data, and this second peak cannot be gated out of the sample. Figure 4.2 shows an example of data with this secondary peak. Though the exact cause of this issue remains to be seen, it can potentially be attributed to a number of factors. First, it is possible that this secondary fluorescent peak is caused by protein nonspecifically binding to the membrane. Because the SNAP-25 GFP construct is biotinylated and biotin is hydrophobic, the biotin could also be nonspecifically interacting with the membrane. Moving towards the SNAP-25 T-Sapphire protein construct (which is not biotinylated) will help to decrease the likeliness of the protein nonspecifically interacting with the membrane. Second, it is also possible that the SNAP-25 protein is crosslinking and the second peak is due to aggregation. In this case, it is necessary to optimize the protein reduction during purification and subsequent conjugation to the lipid-coated microspheres under reduction conditions. Third, it is also possible that degradation of the lipid membrane is occurring. In order to check on this, we must incorporate a fluorescently-labeled lipid control into the protocol. We can measure the fluorescence of these lipid-coated beads at each time point in the protocol to ensure that the membrane is remaining stable throughout the entire assay.

Despite this second peak, however, the fluorescence intensity still clearly decreases with addition of the protease, indicating that the assay is working.

www.manaraa.com

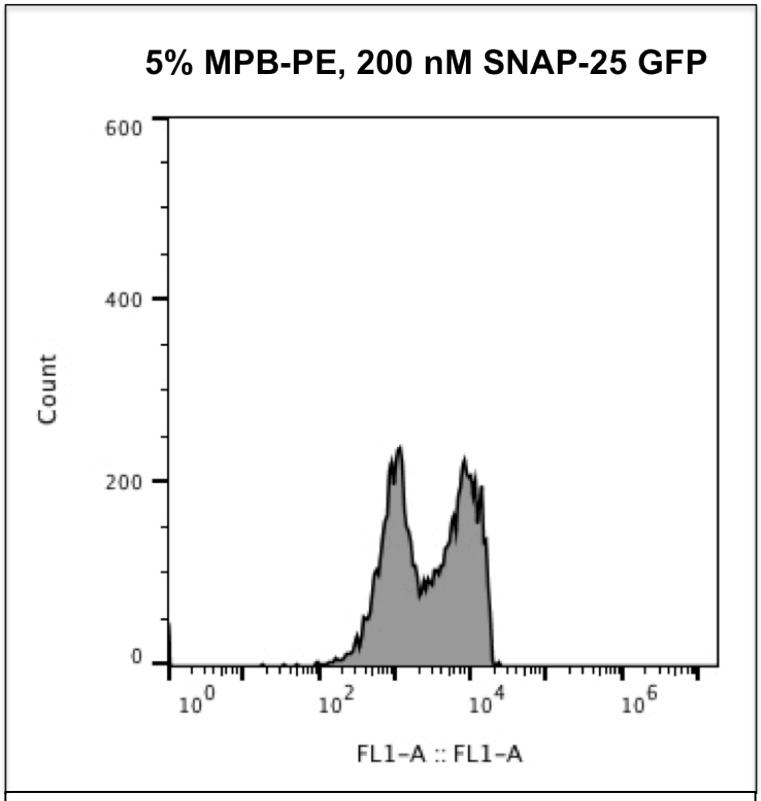

Figure 4.2 Sample containing 5% MPB-PE and 95% POPC in the lipid membrane and incubated with 200 nM of SNAP-25 GFP. Fluorescence intensity is on the x-axis, and count is on the y-axis.

www.manaraa.com

The study of toxin action on membrane-bound substrates in a physiologically relevant environment has many important broader impacts, and the eventual goal of this work is to explore these possibilities. First, due to the extremely fast analysis time of flow-based assay platforms, this assay design is capable of high throughput screening for drug discovery. Secondly, because the current antitoxin treatment for botulism is membrane impermeable and therefore cannot reverse existing paralysis, drug discovery is key for developing more effective treatments. The presence of a membrane in our assay more accurately models a biological system, which is an important factor for drug screening and can lead to more effective treatments. Third, this flow-based assay has multiplexing capability, which allows for cross-reactivity studies. Again, the presence of a membrane may be an important factor in studying the enzymatic activity of the toxin on its membrane-bound substrates. Finally, the membrane-based platform we developed can potentially be used to study other toxins and their activity in a more physiologically relevant environment than that previously employed in microsphere-based assays.

www.manaraa.com

Appendix

FULL-LENGTH CONSTRUCTS OF SNAP-25 GFP AND SNAP-25 T-SAPPHIRE

Full-Length Biotinylated SNAP-25 GFP Plasmid in the Pinpoint Xa-1 Vector

ATGAAACTGAAGGTAACAGTCAACGGCACTGCGTATGACGTTGACGTTGACGTCGACAAGTCACACGAAAACCCGATGGGCACCA
TCCTGTTCGGCGGCGGCACCGGCGGCGCGCCGGCACCGGCAGCAGGTGGCGCAGGCGCCGGTAAGGCCGGAGAGGGCGAGATTCC
CGCTCCGCTGGCCGGCACCGTCTCCAAGATCCTCGTGAAGGAGGGTGACACGGTCAAGGCTGGTCAGACCGTGCTCGTTCTCGAG
GCCATGAAGATGGAGACCGAGATCAACGCTCCCACCGACGGCAAGGTCGAGAAGGTCCTGGTCAAGGAGCGTGACGCGGTGCAGG
GCGGTCAGGGTCTCATCAAGATCGGGGATCTCGAGCTCATGGCCGAAGACGCAGACATGCGCAATGAGCTGGAGGAGATGCAGCG
AAGGGCTGACCAGTTGGCTGATGAGTCGCTGGAAAGCACCCGTCGTATGCTGCAACTGGTTGAAGAGAGTAAAGATGCTGGTATC
AGGACTTTGGTTATGTTGGATGAACAAGGAGAACAACTCGATCGTGTCGAAGAAGGCATGAACCATATCAACCAAGACATGAAGG
AGGCTGAGAAAAATTTAAAAGATTTAGGGAAATGCTGTGGCCTTTTCATATGTCCTTGTAACAAGCTTAAATCAAGTGATGCTTA
CAAAAAAGCCTGGGGCAATAATCAGGACGGAGTGGTGGCCAGCCAGCCTGCTCGTGTAGTGGACGAACGGGAGCAGATGGCCATC
AGTGGCGGCTTCATCCGCAGGGTAACAAATGATGCCCGAGAAAATGAAATGGATGAAAACCTAGAGCAGGTGAGCGGCATCATCG
GGAACCTCCGTCACATGGCCCTGGATATGGGCAATGAGATCGATACACAGAATCGCCAGATCGACAGGATCATGGAGAAGGCTGA
TTCCAACAAAACCAGAATTGATGAGGCCAACCAACGTGCAACAAAGATGCTGGGAAGTGGGCGGATCCACCGGCCGGTCGCCACC
ATGGTGAGCAAGGGCGAGGAGCTGTTCACCGGGGTGGTGCCCATCCTGGTCGAGCTGGACGGCGACGTAAACGGCCACAAGTTCA
GCGTGTCCGGCGAGGGCGAGGGCGATGCCACCTACGGCAAGCTGACCCTGAAGTTCATCTGCACCACCGGCAAGCTGCCCGTGCC
CTGGCCCACCCTCGTGACCACCCTGACCTACGGCGTGCAGTGCTTCAGCCGCTACCCCGACCACATGAAGCAGCACGACTTCTTC
AAGTCCGCCATGCCCGAAGGCTACGTCCAGGAGCGCACCATCTTCTTCAAGGACGACGGCAACTACAAGACCCGCGCCGAGGTGA
AGTTCGAGGGCGACACCCTGGTGAACCGCATCGAGCTGAAGGGCATCGACTTCAAGGAGGACGGCAACATCCTGGGGCACAAGCT
GGAGTACAACTACAACAGCCACAACGTCTATATCATGGCCGACAAGCAGAAGAACGGCATCAAGGTGAACTTCAAGATCCGCCAC
AACATCGAGGACGGCAGCGTGCAGCTCGCCGACCACTACCAGCAGAACACCCCCATCGGCGACGGCCCCGTGCTGCTGCCCGACA
ACCACTACCTGAGCACCCAGTCCGCCCTGAGCAAAGACCCCAACGAGAAGCGCGATCACATGGTCCTGCTGGAGTTCGTGACCGC
CGCCGGGATCACTCTCGGCATGGACGAGCTGTACAAGTAAAGCGGCCGCGATCTGGTTCTATAGTGTCACCTAAATCGTATGTGT
ATGATACATAAGGTTATGTATTAATTGTAGCCGCGTTCTAACGACAATATGTCCATATGGTGCACTCTCAGTACAATCTGCTCTG
ATGCCGCATAGTTAAGCCAGCCCCGACACCCGCCAACACCCGCTGACGCGCCCTGACGGGCTTGTCTGCTCCCGGCATCCGCTTA
CAGACAAGCTGTGACCGTCTCCGGGAGCTGCATGTGTCAGAGGTTTTCACCGTCATCACCGAAACGCGCGAGACGAAAGGGCCTC
GTGATACGCCTATTTTTATAGGTTAATGTCATGATAATAATGGTTTCTTAGACGTCAGGTGGCACTTTTCGGGGAAATGTGCGCG
GAACCCCTATTTGTTTATTTTTCTAAATACATTCAAATATGTATCCGCTCATGAGACAATAACCCTGATAAATGCTTCAATAATA
TTGAAAAAGGAAGAGTATGAGTATTCAACATTTCCGTGTCGCCCTTATTCCCTTTTTTGCGGCATTTTGCCTTCCTGTTTTTGCT
CACCCAGAAACGCTGGTGAAAGTAAAAGATGCTGAAGATCAGTTGGGTGCACGAGTGGGTTACATCGAACTGGATCTCAACAGCG
GTAAGATCCTTGAGAGTTTTCGCCCCGAAGAACGTTTTCCAATGATGAGCACTTTTAAAGTTCTGCTATGTGGCGCGGTATTATC
CCGTATTGACGCCGGGCAAGAGCAACTCGGTCGCCGCATACACTATTCTCAGAATGACTTGGTTGAGTACTCACCAGTCACAGAA
AAGCATCTTACGGATGGCATGACAGTAAGAGAATTATGCAGTGCTGCCATAACCATGAGTGATAACACTGCGGCCAACTTACTTC
TGACAACGATCGGAGGACCGAAGGAGCTAACCGCTTTTTTGCACAACATGGGGGATCATGTAACTCGCCTTGATCGTTGGGAACC
GGAGCTGAATGAAGCCATACCAAACGACGAGCGTGACACCACGATGCCTGTAGCAATGGCAACAACGTTGCGCAAACTATTAACT
GGCGAACTACTTACTCTAGCTTCCCGGCAACAATTAATAGACTGGATGGAGGCGGATAAAGTTGCAGGACCACTTCTGCGCTCGG
CCCTTCCGGCTGGCTGGTTTATTGCTGATAAATCTGGAGCCGGTGAGCGTGGGTCTCGCGGTATCATTGCAGCACTGGGGCCAGA
TGGTAAGCCCTCCCGTATCGTAGTTATCTACACGACGGGGAGTCAGGCAACTATGGATGAACGAAATAGACAGATCGCTGAGATA
GGTGCCTCACTGATTAAGCATTGGTAACTGTCAGACCAAGTTTACTCATATATACTTTAGATTGATTTAAAACTTCATTTTTAAT
TTAAAAGGATCTAGGTGAAGATCCTTTTTGATAATCTCATGACCAAAATCCCTTAACGTGAGTTTTCGTTCCACTGAGCGTCAGA
CCCCGTAGAAAAGATCAAAGGATCTTCTTGAGATCCTTTTTTTCTGCGCGTAATCTGCTGCTTGCAAACAAAAAAACCACCGCTA
CCAGCGGTGGTTTGTTTGCCGGATCAAGAGCTACCAACTCTTTTTCCGAAGGTAACTGGCTTCAGCAGAGCGCAGATACCAAATA
CTGTTCTTCTAGTGTAGCCGTAGTTAGGCCACCACTTCAAGAACTCTGTAGCACCGCCTACATACCTCGCTCTGCTAATCCTGTT
ACCAGTGGCTGCTGCCAGTGGCGATAAGTCGTGTCTTACCGGGTTGGACTCAAGACGATAGTTACCGGATAAGGCGCAGCGGTCG
GGCTGAACGGGGGGTTCGTGCACACAGCCCAGCTTGGAGCGAACGACCTACACCGAACTGAGATACCTACAGCGTGAGCTATGAG
AAAGCGCCACGCTTCCCGAAGGGAGAAAGGCGGACAGGTATCCGGTAAGCGGCAGGGTCGGAACAGGAGAGCGCACGAGGGAGCT
TCCAGGGGGAAACGCCTGGTATCTTTATAGTCCTGTCGGGTTTCGCCACCTCTGACTTGAGCGTCGATTTTTGTGATGCTCGTCA
GGGGGGCGGAGCCTATGGAAAAACGCCAGCAACGCGGCCTTTTTACGGTTCCTGGCCTTTTGCTGGCCTTTTGCTCACATGTTCT
TTCCTGCGTTATCCCCTGATTCTGTGGATAACCGTATTACCGCCTTTGAGTGAGCTGATACCGCTCGCCGCAGCCGAACGACCGA
GCGCAGCGAGTCAGTGAGCGAGGAAGCGGAAGAGCGCCCAATACGCAAACCGCCTCTCCCCGCGCGTTGGCCGATTCATTAATGC
AGGTTAACCTGGCTTATCGAAATTAATACGACTCACTATAGGGAGACCGGCCTCGAGCAGCAAGGAGATGGCGCCCAACAGTCCC
CCGGCCACGGGGCCTGCCACCATACCCACGCCGAAACAAGCGCTCATGAGCCCGAAGTGGCGAGCCCGATCTTCCCCATCGGTGA
TGTCGGCGATATAGGCGCCAGCAACCGCACCTGTGGCGCCGGTGATGCCGGCCACGATGCGTCCGGCGTAGAGGATCGATCCGGG
CTTATCGACTGCACGGTGCACCAATGCTTCTGGCGTCAGGCAGCCATCGGAAGCTGTGGTATGGCTGTGCAGGTCGTAAATCACT
GCATAATTCGTGTCGCTCAAGGCGCACTCCCGTTCTGGATAATGTTTTTTGCGCCGACATCATAACGGTTCTGGCAAATATTCTG
AAATGAGCTGTTGACAATTAATCATCGGCTCGTATAATGTGTGGAATTGTGAGCGGATAACAATTTCACACAGGAAACAGAATTC
CCAGCTTGGCTGCAGAACCATTCCATTCGTTGATCCGGGAGTAACTCAC

www.manaraa.com

Full-Length SNAP-25 T-Sapphire Plasmid in the pET-15b Vector

ttcttgaagacgaaagggcctcgtgatacgcctatttttataggttaatgtcatgataataatggtttcttagacgtcaggtggcact
tttcggggaaatgtgcgcggaacccctatttgtttatttttctaaatacattcaaatatgtatccgctcatgagacaataaccctgat
aaatgcttcaataatattgaaaaaggaagagtatgagtattcaacatttccgtgtcgcccttattccctttttgcggcattttgcct
tcctgtttttgctcacccagaaacgctggtgaaagtaaaagatgctgaagatcagttgggtgcacgagtgggttacatcgaactggat
ctcaacagcggtaagatccttgagagttttcgccccgaagaacgttttccaatgatgagcacttttaaagttctgctatgtggcgcgg
tattatcccgtgttgacgccgggcaagagcaactcggtcgccgcatacactattctcagaatgacttggttgagtactcaccagtcac
agaaaagcatcttacggatggcatgacagtaagagaattatgcagtgctgccataaccatgagtgataacactgcggccaacttactt
ctgacaacgatcggaggaccgaaggagctaaccgcttttttgcacaacatgggggatcatgtaactcgccttgatcgttgggaaccgg
agctgaatgaagccataccaaacgacgagcgtgacaccacgatgcctgcagcaatggcaacaacgttgcgcaaactattaactggcga
actacttactctagcttcccggcaacaattaatagactggatggaggcggataaagttgcaggaccacttctgcgctcggcccttccg
gctggctggtttattgctgataaatctggagccggtgagcgtgggtctcgcggtatcattgcagcactggggccagatggtaagccct
cccgtatcgtagttatctacacgacggggagtcaggcaactatggatgaacgaaatagacagatcgctgagataggtgcctcactgat
taagcattggtaactgtcagaccaagtttactcatatatactttagattgatttaaaacttcatttttaatttaaaaggatctaggtg
aagatccttttgataatctcatgaccaaaatcccttaacgtgagttttcgttccactgagcgtcagaccccgtagaaaagatcaaag
gatcttcttgagatcctttttttctgcgcgtaatctgctgcttgcaaacaaaaaaaccaccgctaccagcggtggtttgtttgccgga
tcaagagctaccaactctttttccgaaggtaactggcttcagcagagcgcagataccaaatactgtccttctagtgtagccgtagtta
ggccaccacttcaagaactctgtagcaccgcctacatacctcgctctgctaatcctgttaccagtggctgctgccagtggcgataagt
cgtgtcttaccgggttggactcaagacgatagttaccggataaggcgcagcggtcgggctgaacgggggttcgtgcacacagcccag
cttggagcgaacgacctacaccgaactgagatacctacagcgtgagctatgagaaagcgccacgcttcccgaagggagaaaggcggac
aggtatccggtaagcggcagggtcggaacaggagagcgcacgagggagcttccagggggaaacgcctggtatctttatagtcctgtcg
ggtttcgccacctctgacttgagcgtcgatttttgtgatgctcgtcaggggggcggagcctatggaaaaacgccagcaacgcggcctt
tttacggttcctggccttttgctggccttttgctcacatgttctttcctgcgttatcccctgattctgtggataaccgtattaccgcc
tttgagtgagctgataccgctcgccgcagccgaacgaccgagcgcagcgagtcagtgagcgaggaagcggaagagcgcctgatgcggt
attttctccttacgcatctgtgcggtatttcacaccgcatatatggtgcactctcagtacaatctgctctgatgccgcatagttaagc
cagtatacactccgctatcgctacgtgactgggtcatggctgcgccccgacacccgccaacacccgctgacgcgccctgacgggcttg
tctgctcccggcatccgcttacagacaagctgtgaccgtctccgggagctgcatgtgtcagaggttttcaccgtcatcaccgaaacgc
gcgaggcagctgcggtaaagctcatcagcgtggtcgtgaagcgattcacagatgtctgcctgttcatccgcgtccagctcgttgagtt
tctccagaagcgttaatgtctggcttctgataaagcgggccatgttaagggcggtttttcctgtttggtcactgatgcctccgtgta
agggggatttctgttcatgggggtaatgataccgatgaaacgagagaggatgctcacgatacgggttactgatgatgaacatgcccgg
ttactggaacgttgtgagggtaaacaactggcggtatggatgcggcgggaccagagaaaaatcactcagggtcaatgccagcgcttcg
ttaatacagatgtaggtgttccacagggtagccagcagcatcctgcgatgcagatccggaacataatggtgcagggcgctgacttccg
cgtttccagactttacgaaacacggaaaccgaagaccattcatgttgttgctcaggtcgcagacgttttgcagcagcagtcgcttcac
gttcgctcgcgtatcggtgattcattctgctaaccagtaaggcaaccccgccagcctagccgggtcctcaacgacaggagcacgatca
tgcgcacccgtggccaggacccaacgctgcccgagatgcgccgcgtgcggctgctggagatggcggacgcgatggatatgttctgcca
agggttggtttgcgcattcacagttctccgcaagaattgattggctccaattcttggagtggtgaatccgttagcgaggtgccgccgg
cttccattcaggtcgaggtggcccggctccatgcaccgcgacgcaacgcggggaggcagacaaggtatagggcggcgcctacaatcca
tgccaacccgttccatgtgctcgccgaggcggcataaatcgccgtgacgatcagcggtccagtgatcgaagttaggctggtaagagcc
gcgagcgatccttgaagctgtccctgatggtcgtcatctacctgcctggacagcatggcctgcaacgcgggcatcccgatgccgccgg
aagcgagaagaatcataatggggaaggccatccagcctcgcgtcgcgaacgccagcaagacgtagcccagcgcgtcggccgccatgcc
ggcgataatggcctgcttctcgccgaaacgtttggtggcgggaccagtgacgaaggcttgagcgagggcgtgcaagattccgaataacc
gcaagcgacaggccgatcatcgtcgcgctccagcgaaagcggtcctcgccgaaaatgacccagagcgctgccggcacctgtcctacga
gttgcatgataaagaagacagtcataagtgcggcgacgatagtcatgccccgcgcccaccggaaggagctgactgggttgaaggctct
caagggcatcggtcgagatcccggtgcctaatgagtgagctaacttacattaattgcgttgcgctcactgcccgctttccagtcggga
aacctgtcgtgccagctgcattaatgaatcggccaacgcgcggggagaggcggtttgcgtattgggcgccagggtggttttttcttttc
accagtgagacgggcaacagctgattgcccttcaccgcctggccctgagagagttgcagcaagcggtccacgctggtttgccccagca
ggcgaaaatcctgtttgatggtggttaacggcgggatataacatgagctgtcttcggtatcgtcgtatcccactaccgagatatccgc
accaacgcgcagcccggactcggtaatggcgcgcattgcgcccagcgccatctgatcgttggcaaccagcatcgcagtgggaacgatg
ccctcattcagcatttgcatggtttgttgaaaaccggacatggcactccagtcgccttcccgttccgctatcggctgaatttgattgc
gagtgagatatttatgccagccagccagacgcagacgcgccgagacagaacttaatgggcccgctaacagcgcgatttgctggtgacc
caatgcgaccagatgctccacgcccagtcgcgtaccgtcttcatgggagaaaataatactgttgatgggtgtctggtcagagacatca
agaaataacgccggaacattagtgcaggcagcttccacagcaatggcatcctggtcatccagcggatagttaatgatcagcccactga
cgcgttgcgcgagaagattgtgcaccgccgctttacaggcttcgacgccgcttcgttctaccatcgacaccaccacgctggcacccag
ttgatcggcgcgagatttaatcgccgcgacaatttgcgacggcgcgtgcagggccagactggaggtggcaacgccaatcagcaacgac
tgtttgcccgccagttgttgtgccacgcggttgggaatgtaattcagctccgccatcgccgcttccacttttcccgcgttttcgcag
aaacgtggctggcctggttcaccacgcgggaaacggtctgataagagacaccggcatactctgcgacatcgtataacgttactggttt
cacattcaccaccctgaattgactctcttccgggcgctatcatgccataccgcgaaaggttttgcgccattcgatggtgtccgggatc
tcgacgctctcccttatgcgactcctgcattaggaagcagcccagtagtaggttgaggccgttgagcaccgccgccgcaaggaatggt
gcatgcaaggagatggcgcccaacagtcccccggccacggggcctgccaccatacccacgccgaaacaagcgctcatgagcccgaagt
ggcgagcccgatcttccccatcggtgatgtcggcgatataggcgccagcaaccgcacctgtggcgccggtgatgccggccacgatgcg
tccggcgtagaggatcgagatctcgatcccgcgaaattaatacgactcactatagggaattgtgagcggataacaattcccctctag
aaataattttgtttaactttaagaaggagatataccatgggcagcagccatcatcatcatcacagcagcggcctggtgccgcgcg
gcagccat...

www.manaraa.com

```
...ATGAAACTGAAAGTGACGGTGAACGGCACGGCATACGATGTTGATGTCGATGTTGATAAAAGCCACGAAAAT
CCGATGGGCACGATCCTGTTTGGCGGTGGCACCGGTGGCGCACCGGCTCCGGCGGCCGGTGGCGCGGGTGCCGGC
AAAGCCGGTGAAGGCGAAATTCCGGCACCGCTGGCTGGCACGGTCAGCAAAATCCTGGTGAAAGAAGGCGATACC
GTGAAAGCCGGTCAGACGGTGCTGGTTCTGGAAGCTATGAAAATGGAAACCGAAATTAACGCGCCGACGGATGGC
AAAGTTGAAAAAGTCCTGGTGAAAGAACGTGATGCCGTCCAGGGTGGCCAAGGTCTGATTAAAATCGGTGATCTG
GAACTGATCGAAGGTCGTATGGCGGAAGATGCCGACATGCGCAATGAACTGGAAGAAATGCAGCGTCGCGCAGAT
CAACTGGCTGACGAATCACTGGAATCGACCCGTCGCATGCTGCAACTGGTGGAAGAAAGTAAAGATGCAGGTATT
CGCACGCTGGTTATGCTGGATGAACAGGGCGAACAACTGGACCGTGTCGAAGAAGGTATGAACCATATTAATCAG
GACATGAAAGAAGCGGAGAAAAAACCTGAAAGACCTGGGCAAATGCTGTGGTCTGTTCATCTGCCCGTGTAATAAA
CTGAAAAGCTCTGACGCGTATAAGAAAGCGTGGGGCAACAATCAGGATGGTGTGGTTGCATCGCAACCGGCTCGT
GTCGTGGATGAACGCGAACAGATGGCTATTAGCGGTGGCTTTATCCGTCGCGTTACCAACGATGCGCGCGAAAAT
GAAATGGACGAAAACCTGGAACAGGTGTCCGGCATTATCGGTAACCTGCGTCACATGGCTCTGGATATGGGCAAT
GAAATTGACACCCAGAACCGTCAAATTGATCGCATCATGGAAAAAGCCGACTCTAATAAAACCCGTATTGATGAA
GCGAACCAGCGCGCCACGAAAATGCTGGGTTCCGGCCGTATCCATCGTCCGGTGGCAACGATGGTGTCAAAAGGC
GAAGAACTGTTTACGGGTGTTGTCCCGATTCTGGTTGAACTGGATGGCGACGTCAATGGTCACAAATTCAGTGTT
TCCGGTGAAGGCGAAGGTGATGCAACCTACGGCAAACTGACGCTGAAATTTATCTGCACCACCGGTAAACTGCCG
GTGCCGTGGCCGACCCTGGTTACCACGTTTTCTTATGGCGTTATGGTCTTCGCCCGTTACCCGGATCACATGAAA
CAGCACGACTTTTTCAAAAGTGCAATGCCGGAAGGCTACGTTCAAGAACGTACCATTTTCTTTAAAGATGACGGT
AACTACAAAACCCGCGCGGAAGTCAAATTCGAAGGCGATACGCTGGTGAATCGTATCGAACTGAAAGGTATCGAT
TTCAAAGAAGACGGCAACATCCTGGGTCATAAACTGGAATATAACTTCAATAGCCACAATGTGTACATTATGGCC
GATAAACAGAAAAATGGTATCAAAGCAAACTTCAAAATCCGCCATAACATCGAAGACGGTGGCGTTCAACTGGCG
GATCACTATCAGCAAAATACCCCGATTGGTGATGGTCCGGTGCTGCTGCCGGATAACCATTACCTGAGCATCCAG
TCTAAACTGAGTAAAGATCCGAATGAAAAACGTGACCACATGGTGCTGCTGGAATTTGTTACGGCGGCGGGTATT
ACGCTGGGTATGGACGAACTGTATAAATGActcgaggatccggctgctaacaaagcccgaaaggaagctgagttg
gctgctgccaccgctgagcaataactagcataaccccttggggcctctaaacgggtcttgaggggttttttgctg
aaaggaggaactatatccggatatcccgcaagaggcccggcagtaccggcataaccaagcctatgcctacagcat
ccagggtgacggtgccgaggatgacgatgagcgcattgttagatttcatacacggtgcctgactgcgttagcaat
ttaactgtgataaactaccgcattaaagcttatcgatgataagctgtcaaacatgagaa
```

www.manaraa.com

REFERENCES

[1] Cai S., Singh B. R. & Sharma S. Botulism diagnostics: from clinical symptoms to in vitro assays. *Crit. Rev. Microbiol.* **33,** 109–125 (2007).

[2] Saunders M. J., Graves S. W., Sklar L. A., Oprea T. I. & Edwards B. S. High-throughput multiplex flow cytometry screening for botulinum neurotoxin type a light chain protease inhibitors. *Assay Drug Dev. Technol.* **8,** 37–46 (2010).

[3] Jahn R. & Scheller R. H. SNAREs--engines for membrane fusion. *Nat. Rev. Mol. Cell Biol.* **7,** 631–643 (2006).

[4] Sørensen J. B., Matti U., Wei S.-H., Nehring R. B., Voets T., Ashery U., Binz T., Neher E. & Rettig J. The SNARE protein SNAP-25 is linked to fast calcium triggering of exocytosis. *Proc. Natl. Acad. Sci. U. S. A.* **99,** 1627–1632 (2002).

[5] Williamson L. C., Halpern J. L., Montecucco C., Brown J. E. & Neale E. A. Clostridial neurotoxins and substrate proteolysis in intact neurons: Botulinum neurotoxin C acts on synaptosomal-associated protein of 25 kDa. *J. Biol. Chem.* **271,** 7694–7699 (1996).

[6] Chen Y. A. & Scheller R. H. SNARE-mediated membrane fusion. *Nat. Rev. Mol. Cell Biol.* **2,** 98–106 (2001).

[7] Hanson P. I., Roth R., Morisaki H., Jahn R. & Heuser J. E. Structure and conformational changes in NSF and its membrane receptor complexes visualized by quick-freeze/deep-etch electron microscopy. *Cell* **90,** 523–535 (1997).

[8] Lin R. C. & Scheller R. H. Structural organization of the synaptic exocytosis core complex. *Neuron* **19,** 1087–1094 (1997).

[9] Poirier M. A., Xiao W., Macosko J. C., Chan C., Shin Y. K. & Bennett M. K. The synaptic SNARE complex is a parallel four-stranded helical bundle. *Nat. Struct. Biol.* **5,** 765–769 (1998).

[10] Fambrough D. M. Control of acetylcholine receptors in skeletal muscle. *Physiol. Rev.* **59,** 165–227 (1979).

[11] Binz T., Sikorra S. & Mahrhold S. Clostridial neurotoxins: Mechanism of SNARE cleavage and outlook on potential substrate specificity reengineering. *Toxins* **2,** 665–682 (2010).

[12] Liu X., Wang Y., Chen P., Wang Y., Zhang J., Aili D. & Liedberg B. Biofunctionalized gold nanoparticles for colorimetric sensing of botulinum neurotoxin A light chain. *Anal. Chem.* **86,** 2345–2352 (2014).

www.manaraa.com

[13] Turton K., Chaddock J. A. & Acharya K. R. Botulinum and tetanus neurotoxins: Structure, function and therapeutic utility. *Trends in Biochemical Sciences* **27,** 552–558 (2002).

[14] Washbourne P., Pellizzari R., Baldini G., Wilson M. C. & Montecucco C. Botulinum neurotoxin types a and e require the SNARE motif in SNAP-25 for proteolysis. *FEBS Lett.* **418,** 1–5 (1997).

[15] Morgan E., Varro R., Sepulveda H., Ember J. A., Apgar J., Wilson J., Lowe L., Chen R., Shivraj L., Agadir A., Campos R., Ernst D. & Gaur A. Cytometric bead array: A multiplexed assay platform with applications in various areas of biology. *Clinical Immunology* **110,** 252–266 (2004).

[16] Abcam PLC. Flow cytometry guide. 1–7 (2012). at <http://docs.abcam.com/pdf/protocols/Introduction_to_flow_cytometry_May_10.pdf>

[17] Li Y. & Sousa R. Expression and purification of E. coli BirA biotin ligase for in vitro biotinylation. *Protein Expr. Purif.* **82,** 162–167 (2012).

[18] Loranger S. S. & Linder M. E. SNAP-25 traffics to the plasma membrane by a syntaxin-independent mechanism. *J. Biol. Chem.* **277,** 34303–34309 (2002).

[19] Criado M., Gil a, Viniegra S. & Gutiérrez L. M. A single amino acid near the C terminus of the synaptosomeassociated protein of 25 kDa (SNAP-25) is essential for exocytosis in chromaffin cells. *Proc. Natl. Acad. Sci. U. S. A.* **96,** 7256–7261 (1999).

[20] Zapata-Hommer O. & Griesbeck O. Efficiently folding and circularly permuted variants of the Sapphire mutant of GFP. *BMC Biotechnol.* **3,** 5 (2003).

[21] Zhu J. Development and Kinetic Modeling of Multiplex Microsphere Assays for High-Throughput Discovery of Protease Active Small Molecule Compounds. (University of New Mexico, 2014).

[22] Martin F. J. & Papahadjopoulos D. Irreversible coupling of immunoglobulin fragments to preformed vesicles. An improved method for liposome targeting. *J. Biol. Chem.* **257,** 286–288 (1982).

[23] Chemburu S., Fenton K., Lopez G. P. & Zeineldin R. Biomimetic silica microspheres in biosensing. *Molecules* **15,** 1932–1957 (2010).

[24] Hermanson G. T. *Bioconjugate Techniques*. (Academic Press, 2013).

www.manaraa.com

[25] Piyasena M. E., Zeineldin R., Fenton K., Buranda T. & Lopez G. P. Biosensors based on release of compounds upon disruption of lipid bilayers supported on porous microspheres. *Biointerphases* **3,** 38 (2008).

[26] Savarala S., Ahmed S., Ilies M. A. & Wunder S. L. Formation and colloidal stability of DMPC supported lipid bilayers on SiO2 nanobeads. *Langmuir* **26,** 12081–12088 (2010).

[27] Nair P. M., Salaita K., Petit R. S. & Groves J. T. Using patterned supported lipid membranes to investigate the role of receptor organization in intercellular signaling. *Nat. Protoc.* **6,** 523–539 (2011).

[28] Olsen J. V, Ong S.-E. & Mann M. Trypsin cleaves exclusively C-terminal to arginine and lysine residues. *Mol. Cell. Proteomics* **3,** 608–614 (2004).

[29] Sakaba T., Stein A., Jahn R. & Neher E. Distinct Kinetic Changes in Neurotransmitter Release after SNARE Protein Cleavage Author(s): Takeshi Sakaba, Alexander Stein, Reinhard Jahn and Erwin Neher Source: **309,** 491–494 (2015).

[30] Cornejo J. DEVELOPMENT OF SURFACE BASED PLATFORMS FOR BIOMOLECULAR RECOGNITION AND PROTEASE ASSAYS. (University of New Mexico, 2013).

[31] Avanti Polar Lipids, Inc. (2015). at <http://www.avantilipids.com/>

www.manaraa.com